

CORRELATION OF MECHANICAL BEHAVIOR OF ENDOPELVIC FASCIA  
VERSUS VARIABLES IN AQUISITION OF SPECIMENS

A THESIS

Presented to

The Faculty of the Division of Graduate Studies

By

Kenneth Ray Jones

In Partial Fulfillment

of the Requirements for the Degree


Master of Science in Engineering Science and Mechanics

Georgia Institute of Technology


September, 1977

CORRELATION OF MECHANICAL BEHAVIOR OF ENDOPELVIC FASCIA  
VERSUS VARIABLES IN AQUISITION OF SPECIMENS


Approved



Hyland Y. L. Chen, Chairman



Raymond P. Vito



Stephen L. Passman

11-21-77

Date approved by Chairman

To my wife, Lisa, for her encouragement and support

# ACKNOWLEDGEMENTS

I am deeply appreciative of the time, counsel and friendship given to me by my advisor, Professor Hyland Yu-Liang Chen. He has granted me the opportunity to learn, which is the essence of teaching.

I would like to thank the members of my Reading Committee, Dr. Stephen L. Passman and Dr. Raymond P. Vito, for their recommendations concerning the wording of the thesis. They have gone out of their way to be helpful.

I am grateful to Dr. A.C. Richardson for introducing me to the problem of pelvic relaxation. His advice and assistance has been invaluable.

I would like to thank Mr. John Lee and Mr. Steve P. Benolst for their work on the computer control and electronic gadgetry.

I am grateful to Mr. Richard T. Hart for teaching me to use the Alphasatron and for many valuable discussions.

Thanks are due to Mr. Bob Badalament for gathering

the specimens and helping me to understand the anatomy of pelvic relaxation.

The nonlinear curve fit program used to reduce the data was written by Mr. John Fay.

I thank the Graduate Division for waiving certain format requirements so that this thesis could be typed by the Georgia Tech CDC Cyber 74.

## TABLE OF CONTENTS

DEDICATION.....	ii
ACKNOWLEDGMENTS.....	iii
LIST OF TABLES.....	vi
LIST OF ILLUSTRATIONS.....	vii
SUMMARY.....	ix
I. INTRODUCTION.....	1
II. METHOD.....	4
Experimental Apparatus	
Tissue Acquisition	
Preconditioning	
Testing Procedure	
III. RESULTS.....	10
Observations	
Simple Elongation	
Stress-Relaxation	
Ultimate Strength	
Analysis	
Quasilinear Viscoelastic Model	
Elastic Response	
History Dependent Response	
IV. CONCLUSIONS.....	23
APPENDIX.....	27
BIBLIOGRAPHY.....	51

## LIST OF TABLES

Table	Page
1. Tissue Measurements and Ultimate Strength .....	19
2. Simple Elongation Results Using a Nonlinear Curve Fit .....	20
3. Slope of Relaxation .....	21
4. Correlation of $\alpha$ and $\beta$ with Stress-Strain Curves ....	22

## LIST OF ILLUSTRATIONS

Figure	Page
A1. Effect of Strain Rate on Stress-Strain Curve CF163 .....	28
A2. Effect of Strain Rate on Stress-Strain Curve CF164 .....	29
A3. Effect of Strain Rate on Stress-Strain Curve CF167 .....	30
A4. Stress versus Stretch Ratio -CF167 and NF527 .....	31
A5. Stress versus Stretch Ratio -CF163 and CF164 .....	32
A6. Stress versus Stretch Ratio -CM361 and CM362 .....	33
A7. Stress versus Stretch Ratio -CM363 and CM364 .....	34
A8. Stress versus Stretch Ratio -NF521 and NF522 .....	35
A9. Stress versus Stretch Ratio -NF523 and NF524 .....	36
A10. Stress versus Stretch Ratio -NF525 and NF526 .....	37
A11. Secant Elastic Modulus versus Stress - CF163 .....	38
A12. Secant Elastic Modulus versus Stress - CF164 .....	39
A13. Secant Elastic Modulus versus Stress - CF167 .....	40
A14 Secant Elastic Modulus versus Stress CF167 and NF527 .....	41
A15 Secant Elastic Modulus versus Stress CF163 and CF164 .....	42
A16 Secant Elastic Modulus versus Stress CM361 and CM362 .....	43
A17 Secant Elastic Modulus versus Stress CM363 and CM364 .....	44

Figure	Page
A18 Secant Elastic Modulus versus Stress NF521 and NF522 .....	45
A19 Secant Elastic Modulus versus Stress NF523 and NF524 .....	46
A20 Secant Elastic Modulus versus Stress NF525 and NF526 .....	47
A21. Reduced Relaxation Function CF163,CF164,CF167 .....	48
A22. Reduced Relaxation Function CM361,CM362,cM363,CM364 .....	49
A23. Reduced Relaxation Function NF521,NF522,NF523,NF524 .....	50
A24. Reduced Relaxation Function NF525,NF526,NF527 .....	51

## Summary

Specimens of rectus sheath and round ligament of the uterus were tested in uniaxial tension. Simple elongation, relaxation, and ultimate strength tests were performed on 16 tissues from three subjects. The stress-strain behavior is modeled by the equation  $T^e = \beta [e^{\alpha(\epsilon-1)} - 1]$ . The data seems to fit this equation very well. The stress was found to be independent of strain rate in a range from 0.015/sec. to 0.21/sec. The rectus sheath exhibited significant anisotropy. The relaxation behavior and ultimate strength did not appear to be orientation dependent. We could not observe any dependence of the stress-strain behavior, relaxation behavior or ultimate strength on age, race, or sex. The ultimate strength varied from  $0.14 \times 10^6$  Pascals to  $2.14 \times 10^6$  Pascals.

## CHAPTER I

### INTRODUCTION

In order to understand the physiological function of an organ or tissue, it is often necessary to obtain information about its mechanical properties. Recently, medical research in pelvic relaxation has established the need for mechanical data on the behavior of tissues in the female pelvic support structures [17].

"Pelvic relaxation is a general term used to describe all conditions in which the supporting structure in the female pelvis no longer maintains the pelvic organs in their normal position." [11] It is usually found in older women. Most procedures for surgical repair of these conditions are based on the theory that there is a generalized relaxation, or attenuation of the connective tissues comprising the pelvic supports. Surgical repair is needed when extensive stretching leads to herniation or when it disrupts the normal functions of the pelvic organs. General plication techniques to shorten the "elongated" pelvic supports are commonly used.

While pelvic relaxation is "among the commonest

complaints heard daily by all gynecologists. . . . successful vaginal repair is the most difficult type of gynecologic surgery, and even an experienced gynecologist may have failure rates ranging from 25 to 41 per cent." [1] These failure rates are observed to increase with time.

Research in the clinic of Dr. A. C. Richardson of Atlanta has led him to conclude that usually, if not always, pelvic relaxation is the result of an isolated defect or tear in the pelvic support tissues rather than a generalized stretching. Between January, 1971 and October, 1975, 93 operations were performed in which localized defects were found and repaired. Their failure rate was less than 5%. In addition, three of the four failures were evident within six weeks after surgery [17].

In order to analyze the genesis of pelvic relaxation, the following questions need to be answered:

- (1) Which structures provide support for the pelvic organs ?
- (2) What is the geometric configuration of these structures ?
- (3) What are the loads on these structures ?
- (4) What are the mechanical properties of the tissues comprising the pelvic supports ?

(5) What is the histology of these tissues ?

A pilot study has been initiated to study the anatomy of the pelvic supports and the histology of the tissues involved. Preliminary results indicate that several structures provide support for the pelvic organs. Histological studies [18] have shown that endopelvic fascia has a large percentage (over 50%) of smooth muscle. Smooth muscle was found to be predominant in every structure extending from the uterus to the pelvic sidewall.

The purpose of this work was to test specimens of endopelvic fascia to obtain information about the mechanical properties of various tissues in the pelvic support structure. Tissue samples obtained in longitudinal and latitudinal strips were tested in order to observe possible anisotropic behavior. Samples from various sites were tested in order to observe any variation with respect to location in the structure.

## CHAPTER II

### METHOD

#### Apparatus

A revised version of the "Alphatron"[11] was used to perform mechanical tests on the tissues. The existing "Alphatron" is a one-dimensional materials testing device consisting of three components: the mechanical system, the control system and the environmental system.

The mechanical system is a digitally controlled, closed loop servo system. The power train (Torque Systems, model MTE-3323-(24HE) is a DC motor which produces linear displacement by a lead screw (Beaver Precision). The motor is equipped with conventional power supply and analog compensation circuitry. A Fairchild (F-8) microprocessor and accessory firmware in conjunction with an optical encoder in the motor provide digital control of the input to the analog compensation circuits. The Fairchild microprocessor is programmed so that when provided with parameters representing acceleration, velocity, and displacement, it will produce the desired displacement  $d$  with a constant velocity  $v$ . The system will start the motion with an acceleration  $a$  until it achieves velocity  $v$ , maintain  $v$  for

a period of time, then stop with a deceleration of  $a$ .

The control system is a special purpose digital processing unit designed to provide an interactive input mechanism for specifying the parameters to the Fairchild microprocessor.

A Statham Gold Cell was used to measure the force. Various adapters provide the ability to vary the load range from 1.1 Newtons to 222 Newtons. It has a resolution of 0.08 Newtons and frequency response of 180 Hertz. The signal from the Gold Cell was amplified by a strain gage amplifier (Validyne). A Trans-Tek LVDT (Linear Variable Displacement Transducer) was used to measure the displacement in a one centimeter range. It has a resolution of 0.01 Cm and a frequency response of 1000 Hertz. The signal from the LVDT was amplified by a carrier-demodulator amplifier (Validyne). The amplified signals were recorded by an oscillograph (Honeywell Visicorder).

The environmental tank controls the chemical and thermal environment of the specimens. The specimens were immersed in physiological saline solution at 37 C.

### Tissue Acquisition

Tissue samples of various connective tissues of the pelvic supports were obtained from fresh autopsy material. Samples were approximately 0.4 cm wide and of various lengths and thicknesses depending on location and individual. The length and mass of each specimen is listed in Table 1. Tissues were taken from the posterior rectus sheath from above and below the arcuate line, the anterior rectus sheath, and the round ligament of the uterus. At each location in the rectus sheath, one longitudinal strip and one latitudinal strip were cut in order to observe dependence on orientation.

Tissues were frozen between 12 and 48 hours of death and thawed immediately before testing. Studies have shown that freezing does not significantly affect the mechanical properties of many biological tissues [14,15,21,22,23]. Several authors investigating the change in mechanical properties of biological tissues after death have published conflicting results on how long tissues can be considered "fresh" [3,6,19,24]. After thawing, each end of the tissue was sandwiched between two bamboo clamps which were tied securely with surgical silk. Wire hooks were placed through the bamboo clamps. The top hook was attached to the Gold Cell adapter and the other hook was attached to the loading

bar.

In the text, tissues are identified by an alphanumeric code indicating race, sex, age, and tissue type. Tissue types are listed below.

- 1 - Longitudinal posterior rectus sheath  
above the arcuate line
- 2 - Latitudinal posterior rectus sheath  
above the arcuate line
- 3 - Longitudinal posterior rectus sheath  
below the arcuate line
- 4 - Latitudinal posterior rectus sheath  
below the arcuate line
- 5 - Longitudinal anterior rectus sheath
- 6 - Latitudinal anterior rectus sheath
- 7 - Round ligament of the uterus

As an example, CF161 refers to tissue type 1 from a Caucasian female 16 years old.

#### Preconditioning

Data seems to indicate that biological tissues have no natural configuration to which they return after deformation [8,9]. This presents a problem when trying to define a reference length for measuring strain. A common practice is to "precondition" the tissue by stretching it repeatedly until a steady state response is achieved. After preconditioning, the specimen was stretched until a load could be detected. Then, the specimen was shortened until no load was detected. The length was measured and

taken to be the reference length  $l_0$ . The stretch ratio is given as  $l/l_0$ . The tissue is very "soft" at low strain levels. This further complicates determining  $l_0$ . The reference length is probably the least accurate of the quantities measured.

#### Testing Procedure

Three tests were run on each specimen: simple elongation, stress relaxation and ultimate strength.

In the simple elongation test, the specimen was loaded at a constant strain rate to a given strain level. three specimens (CF163, CF164, CF167) were tested at various strain rates in order to observe the effect of the strain rate on stress-strain curves. Hart[11] found no dependence on rate. Our results for the first three specimens agreed with his so all other tissues were tested at one speed (0.188 cm/sec).

In the stress relaxation test, the specimens were stretched from the reference length  $l_0$  to a given length  $l$  at 0.75 cm/sec. Force data was recorded for 1000 seconds.

The final test was the ultimate strength test in which the specimen was stretched at 0.0038 cm/sec until the

stress peaked. After this test the tissue was removed from the apparatus, cut from the clamps, and weighed.

### CHAPTER III

#### RESULTS

##### Observations

Sixteen specimens were tested. During the first test, the specimen pulled out of the clamps. Since no comparisons could be made, data is not presented for specimen CF161 or its companion CF162. In subsequent tests, more care was taken in tying the clamps and they held securely.

##### Simple Elongation

Assuming that the tissue is incompressible and the specimen is prismatic, the Eulerian stress,  $T$ , was calculated as,

$$T = (F)(l_0)(\lambda)/V \quad (1)$$

where  $F$  is the measured force;  $l_0$  is the reference length;  $\lambda$  is the stretch ratio;  $V$  is the volume of the specimen. Assuming that the specimen has a density close to that of water, the volume can be obtained directly from the mass of the specimen.

Plots of the stress  $T$  versus  $\lambda$ , are shown in Figures

A1. - A10. The curves appear to be exponential. The stress-strain curves for the three specimens tested at various rates are shown in Figures A1 - A3. After specimen CF163 was tested at strain rates of 0.022/sec. and 0.043/sec., it was accidentally damaged by overstretching. In Figure A1, we see that the curves for the tests before damage are close and the curves for tests after damage are close. In Figure A2. and Figure A3., we see very little difference in the curves for all four strain rates. These results agree with those of Hart[11].

Stress-strain curves for the other specimens are plotted in Figures A4. - A10. Quantitatively comparing the stress-strain curves of two specimens, we say that the specimen with the higher stress at a given is less compliant. In Figure A4. we see that the round ligament of the 16 year old female is less compliant than that of the 52 year old. In Figures A5. - A10., we see that for the posterior rectus sheath above the arcuate line and the anterior rectus sheath, the latitudinal specimens were less compliant than the longitudinal specimens. In the posterior rectus sheath below the arcuate line, the longitudinal specimens were less compliant.

## Relaxation

The reduced relaxation function was calculated as,

$$G(t) = T(t)/T(0) \quad (2)$$

where  $t=0$  was the time at which the tissue reached the desired stretch  $\lambda_p$ . The values of  $G(t)$  were plotted versus  $t$  on a semilog scale in figures A21 - A24. All tissues apparently continued to relax for the full 17 minutes.

## Ultimate Strength

During the ultimate strength tests, the stress appeared to increase exponentially at first, level off erratically, then decrease slowly. The erratic behavior may have been due to the effects of individual fibers breaking and the load shifting to other fibers, or the effect of local slipping in the clamps. At the maximum force, the tissue appears thinner but no broken fibers were observed. As the tissue continued to stretch, the stress decreased, and broken fibers became apparent. The tissue tore apart as more and more fibers broke. Microscopic examination of specimens during tests may yield important information about what happens to components of the specimen as the stress approaches the yield stress. The ultimate strength for each specimen is listed in Table 1. It is not known whether these stresses correspond to stresses experienced by the

tissues in their physiological function.

### Analysis

Data from mechanical tests on biological tissues is of little value unless we can find a way to make meaningful comparisons between specimens. Much attention has been directed towards the ultimate strength [24]. In trying to understand mechanical aspects of pelvic relaxation, this would seem to be of great importance. However, information which will help us to understand the mechanical behavior in the course leading to the ultimate failure must also be considered. A mathematical model of the mechanical behavior provides the tool to unify our experimental observations, and to use these results to predict the mechanical behavior under a variety of conditions. We would like to have a simple model with few constants to evaluate, that will describe the data. We have observed that the quasilinear-viscoelastic model proposed by Fung[8] appears to meet this criteria.

### The Quasilinear-viscoelastic Model

The quasilinear-viscoelastic model is based on a hypothetical "elastic stress"  $T^e(\lambda)$ , a function of the instantaneous strain, and a linear relaxation law that determines the current stress  $T(t)$  in terms of the history of the "elastic stress". The relaxation function,  $K(\lambda, t)$ ,

is defined to be the history of stress response to a suddenly applied stretch  $\lambda$  written as,

$$\lambda(t) = 1 + (\lambda - 1)H(t) \quad (3)$$

where  $H(t)$  is the Heaviside step function, i.e.,

$$H(t) = \begin{cases} 0 & \text{for } t \leq 0 \\ 1 & \text{for } t > 0 \end{cases} \quad (4)$$

The relaxation behavior as observed by Hart [11] suggests that the relaxation function can be written in the form,

$$K(\lambda, t) = G(t)T^e(\lambda). \quad (5)$$

The reduced relaxation function,  $G(t)$ , is a normalized function of time with the property that,  $G(0) = 1$ . Assuming the superposition principle yields an expression for the stress due to a stretch history  $\lambda(t)$ .

$$\tau(t) = T^e[\lambda(t)] + \int_0^t T^e[\lambda(t-\tau)] \frac{\partial G(\tau)}{\partial \tau} d\tau \quad (6)$$

#### Elastic Response

The "elastic response"  $T^e(\lambda)$  is defined to be the instantaneous stress generated by a suddenly applied stretch  $\lambda$ . Strict measurement of  $T^e(\lambda)$  is impractical because it involves loading at an infinite rate. Increasing the stretch ratio from 1 to  $\lambda$  in a time interval  $\epsilon$ , we can obtain the

stress at  $t=\epsilon$ ,  $T(\epsilon)$ . Fung[8] has shown that, if  $\epsilon \frac{dG(\lambda)}{d\lambda} \ll 1$ , then we can use the approximate relation  $T^e(\lambda) \approx T(\epsilon)$ .

Various equations for the form of the function  $T^e(\lambda)$  for biological tissues have been investigated. Kenedi[12] and Fung[7] have proposed the equation,

$$T^e(\lambda) = \beta [e^{\alpha(\lambda-1)} - 1] \quad (7)$$

In a study comparing seven equations used for biological tissues, Rabkin and Hsu[16] chose equation (7) as best fitting their data for the stress-strain relation of pericardium. The equation has also been used for rabbit mesentery[4,5] and the series element of myocardium[20].

The secant elastic modulus,  $DT/D\lambda$ , was calculated as,

$$\frac{DT}{D\lambda} = \frac{T - T_{i-1}}{\lambda - \lambda_{i-1}} \quad (8)$$

Plots of  $DT/D\lambda$  versus  $T$  are shown in Figures A11. - A20. A linear regression of the data was done to obtain  $\alpha$  and  $\beta$  to fit the linearized equation,

$$\frac{dT}{d\lambda} = \alpha T + \beta \quad (9)$$

The graphs show that there are large errors in  $DT/D\lambda$ . In some cases,  $\beta$  was less than zero. This is physically absurd.

A nonlinear least-squares curve fitting method [2] was used to determine  $\alpha$ 's and  $\beta$ 's to fit equation (7). The values of  $\alpha$  and  $\beta$ , and the RMS errors are listed in Table 2. The RMS errors ranged from 0.015 (NF521) to 0.813 (CF167). Theoretical curves for these two sets of data are plotted on Figures A3. and A8. The curves appear to fit well. It is interesting to note that for the three specimens that were tested for different strain rates is larger for the two higher rates than for the two lower rates. This may be due to changes in the tissue induced by repeated tests. Both parameters seem to vary more between specimens in the older subjects. The parameter varies over three orders of magnitude. This is probably due to its sensitivity to the choice of  $l_0$ .

Neither  $\alpha$  nor  $\beta$  alone is sufficient to compare the compliance of two tissues. Table 4 lists which tissue type of each pair has a larger value of  $\alpha$  and  $\beta$ , and the curve showing less compliance. For tissue types three and four of

the Caucasian male and the Negro female, the less compliant specimen of the pair does not have the larger  $\alpha$  or  $\beta$ . For the other specimens,  $\alpha$  and  $\beta$  correlate directly with compliance.

#### History Dependent Response

We observe from the data that the stress-strain curves are relatively independent of the strain rate. This allows us to employ a continuous relaxation spectrum  $S(\tau)$  [8] to write the reduced relaxation function in the form

$$G(t) = \frac{1 + \int_0^{\infty} S(\tau) e^{-t/\tau} d\tau}{1 + \int_0^{\infty} S(\tau) d\tau} \quad (10)$$

If we choose

$$S(\tau) = C/\tau \quad \text{for } \tau_1 < \tau < \tau_2 \quad (11)$$

$$S(\tau) = 0 \quad \text{for } \tau < \tau_1, \tau_2 < \tau \quad (12)$$

where  $C$  is a constant, we can write,

$$G(t) = \frac{1 + C[E1(t/\tau_2) - E1(t/\tau_1)]}{1 + C \ln(\tau_2/\tau_1)} \quad (13)$$

where

$$E1(z) = \int_z^{\infty} \frac{e^{-t}}{t} dt \quad (14)$$

Following the calculation scheme of Ko[15] and Hart[12], we calculate the reduced relaxation function from the equation

$$G(t) = \frac{1 - C\gamma + C \ln(\tau_2) - C \ln(t)}{1 + C \ln(\tau_2) - C \ln(\tau_1)} \quad (15)$$

where  $\gamma$  (approximately 0.57721) is the Euler constant.

The function  $G(t)$  for a solid with a continuous relaxation spectrum  $S(\tau) = C/\tau$  decreases nearly linearly with  $\ln(t)$  for  $\tau_1 \ll t \ll \tau_2$ . The slope,  $S_r$ , of the straight line approximating this portion of the graph can be written

$$S_r = \frac{dG}{d(\ln t)} = \frac{-C}{1 + C \ln(\tau_2) - C \ln(\tau_1)} \quad (16)$$

Thus we have three parameters,  $c$ ,  $\tau_1$ , and  $\tau_2$  to fit our experimental data. A linear regression of  $G(t)$  versus  $\ln(t)$  was done to obtain values for  $S_r$ . They are shown in Table 3.

Table 1. Tissue Measurements and Ultimate Strength

Specimen	$l_0$ (centimeters)	Mass (grams)	$\lambda_0$	Ultimate Strength ( $\times 10^5$ Pascals)
CF163	1.765	.088	1.06	6.2
CF164	1.004	.155	1.12	3.7
CF167	2.574	.445	1.25	7.0
CM361	2.481	.335	1.85	5.2
CM362	1.448	.141	1.38	14.7
CM363	1.209	.049	1.66	7.8
CM364	0.651	.097	2.87	15.5
NF521	3.136	.168	1.31	12.3
NF522	1.188	.151	1.25	9.7
NF523	1.185	.078	1.58	9.0
NF524	0.672	.061	2.88	21.4
NF525	1.107	.151	2.40	12.2
NF526	1.096	.235	1.44	1.4
NF527	0.509	.071	2.75	9.1

Table 2. Nonlinear Curve Fit Results for Simple Elongation

Specimen	$\alpha$	$\beta$	RMS Error
	(x10 <sup>5</sup> Pascals)		
CF163-1	46.3	0.511	.214
-2	44.2	0.564	.153
-3	27.3	7.82	.420
-4	25.5	12.5	.472
CF164-1	28.2	.0526	.312
-2	30.4	.0257	.179
-3	25.5	.162	.386
-4	26.2	.129	.491
CF167-1	45.4	6.39	.016
-2	44.5	8.97	.022
-3	42.2	12.8	.078
-4	42.5	12.5	.060
CM361	16.9	.031	.642
CM362	89.0	.147	.130
CM363	19.3	128	.280
CM364	27.0	.712	.139
NF521	37.3	5.29	.813
NF522	55.4	95.5	.138
NF523	49.1	1.35	.307
NF524	35.0	3.56	.258
NF525	13.6	.460	.252
NF526	16.0	6.95	.312
NF527	23.7	3.16	.208

Table 3. Slope of Relaxation

Specimen	Sr	$\lambda_r$	r
CF163	-0.024	1.29	-0.953
CF164	-0.025	1.51	-0.997
CF167	-0.027	1.17	-0.996
CM361	-0.030	1.82	-0.659
CM362	-0.027	1.22	-0.997
CM363	-0.032	1.32	-0.995
CM364	-0.051	1.35	-0.894
NF521	-0.029	1.26	-0.873
NF522	-0.048	1.13	-0.865
NF523	-0.036	1.21	-0.870
NF524	-0.026	1.28	-0.871
NF525	-0.040	1.80	-0.877
NF526	-0.036	1.46	-0.887
NF527	-0.042	1.37	-0.896

Table 4. Correlation of  $\alpha$  and  $\beta$  with Stress-Strain Curves

Tissue Pairs	Tissue with larger $\alpha$	Tissue with larger $\beta$	Tissue with less compliance
CF163,4	3	3	3
CM363,4	4	3	3
NF523,4	3	4	3
CM361,2	2	2	2
NF521,2	2	2	2
NF525,6	6	6	6

## CHAPTER IV

### CONCLUSIONS

We have tested 16 specimens from various locations in the connective tissues of the pelvic support structure. The three subjects were of different ages, races, and sexes. Two points should be noted: (1) due to the difficulty in obtaining specimens, we have not done enough tests for our results to be statistically significant, and (2) there are many variables not controlled in our experiments. However, certain trends do appear and we draw conclusions based on these trends.

The proposed mathematical model is intended to provide a vehicle to describe our observations from various tests. It should enable us predict mechanical behavior in a variety of circumstances utilizing data from a few observations.

Simple elongation tests show that for rectus sheath and round ligament of the uterus, the stress increases exponentially with strain. Equation (7) appears to fit our experimental data well, when the nonlinear curve fit method [2] is used. Both  $\sigma$  and  $\epsilon$  are needed for comparing the

compliance of two specimens.

The stress was independent of strain rate in a range from 0.015/sec. to 0.21/sec. This suggests the use of the continuous relaxation spectrum  $S(\tau)$  in the quasilinear-viscoelastic model.

The rectus sheath exhibits significant anisotropy at various locations. The nature of the anisotropy varies from location to location. This will require that a 3-D model of the pelvic supports incorporate a map of the mechanical behavior at each point in the structure. Correlation of histological data with mechanical data may help to clarify the source of the anisotropy [10,24].

Relaxation results showed that the reduced relaxation function did appear to decrease linearly with  $\ln(t)$ , although the fit to a straight line was not very good in a number of tests. We could not observe any gross differences in relaxation behavior with respect to age, race, sex, or orientation.

The ultimate strength results showed a great deal of scatter. We could not observe any dependence on age, race, sex or orientation. Since the ultimate strength tests were

always the last to be performed, the results should be viewed in the light of possible damage due to previous tests. The stresses experienced by these tissues in the body are not known therefore, we do not know if the measured strength is indicative of the strength in vivo.

We observed a decrease in uniformity of mechanical behavior of specimens with age of the subject. This was evident in simple elongation, relaxation, and ultimate strength tests. If this trend is not an artifact due to the larger number of specimens for the older subjects, it would seem to indicate that as tissues age, variations in mechanical properties within the structures increase. These variations may lead to local stress concentrations or local weakening of the structure, increasing the chance of a local failure.

By removing the tissues from the body for testing, we subject them to many mechanical, chemical, osmotic and metabolic changes. It is unreasonable to expect to be able to extrapolate quantitatively from our quantitative results for in vitro tests to the in vivo situation. However, it is plausible to assume that the in vivo and in vitro behavior will at least be qualitatively similar. In this sense, we should be able to use in vitro observations to qualitatively

compare the in vivo behavior of two tissues.

APPENDIX

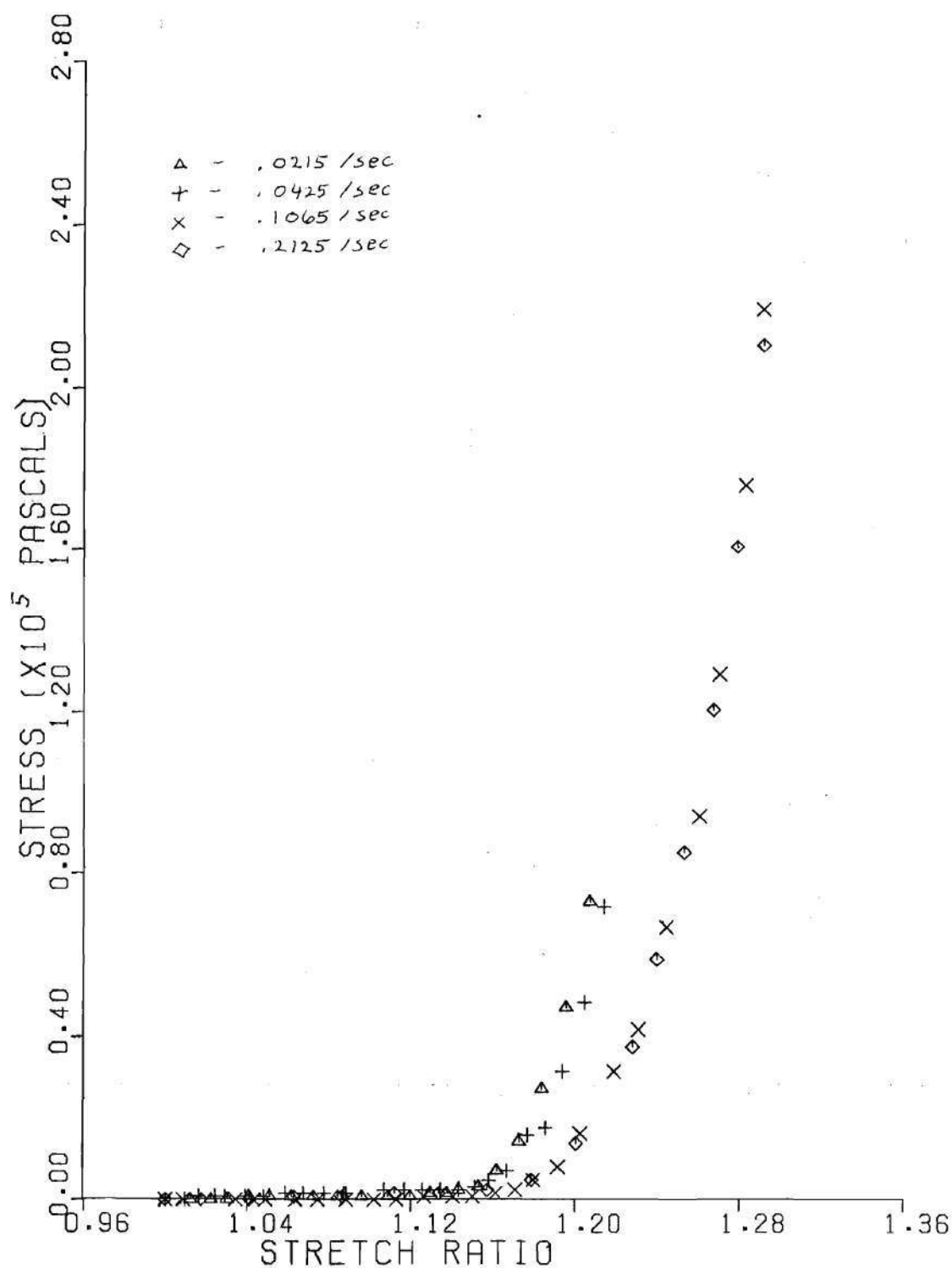


Figure A1. Effect of Strain Rate on Stress-Strain Curve - CF163

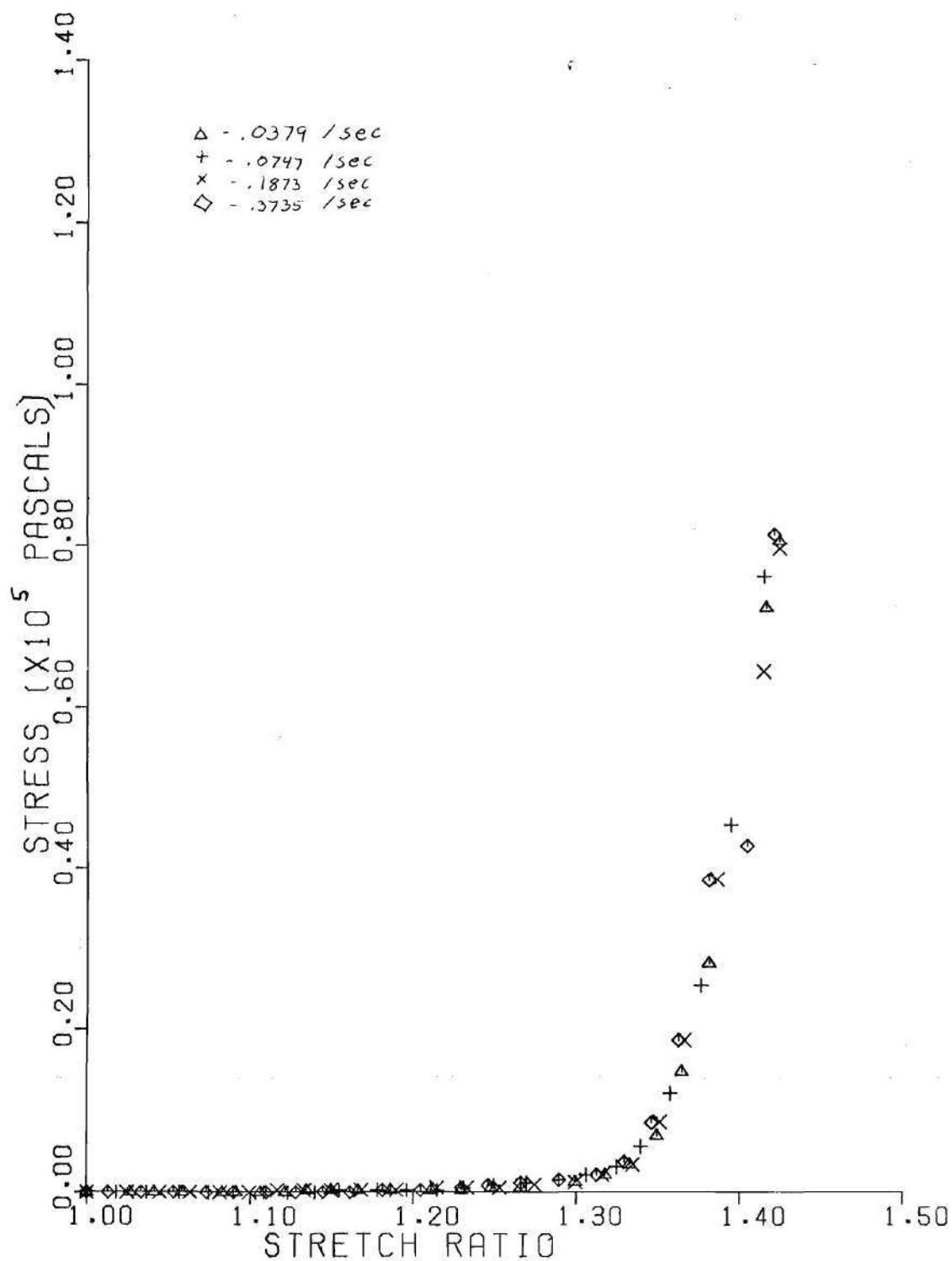


Figure A2. Effect of Strain Rate on Stress-Strain Curve -  
CF164

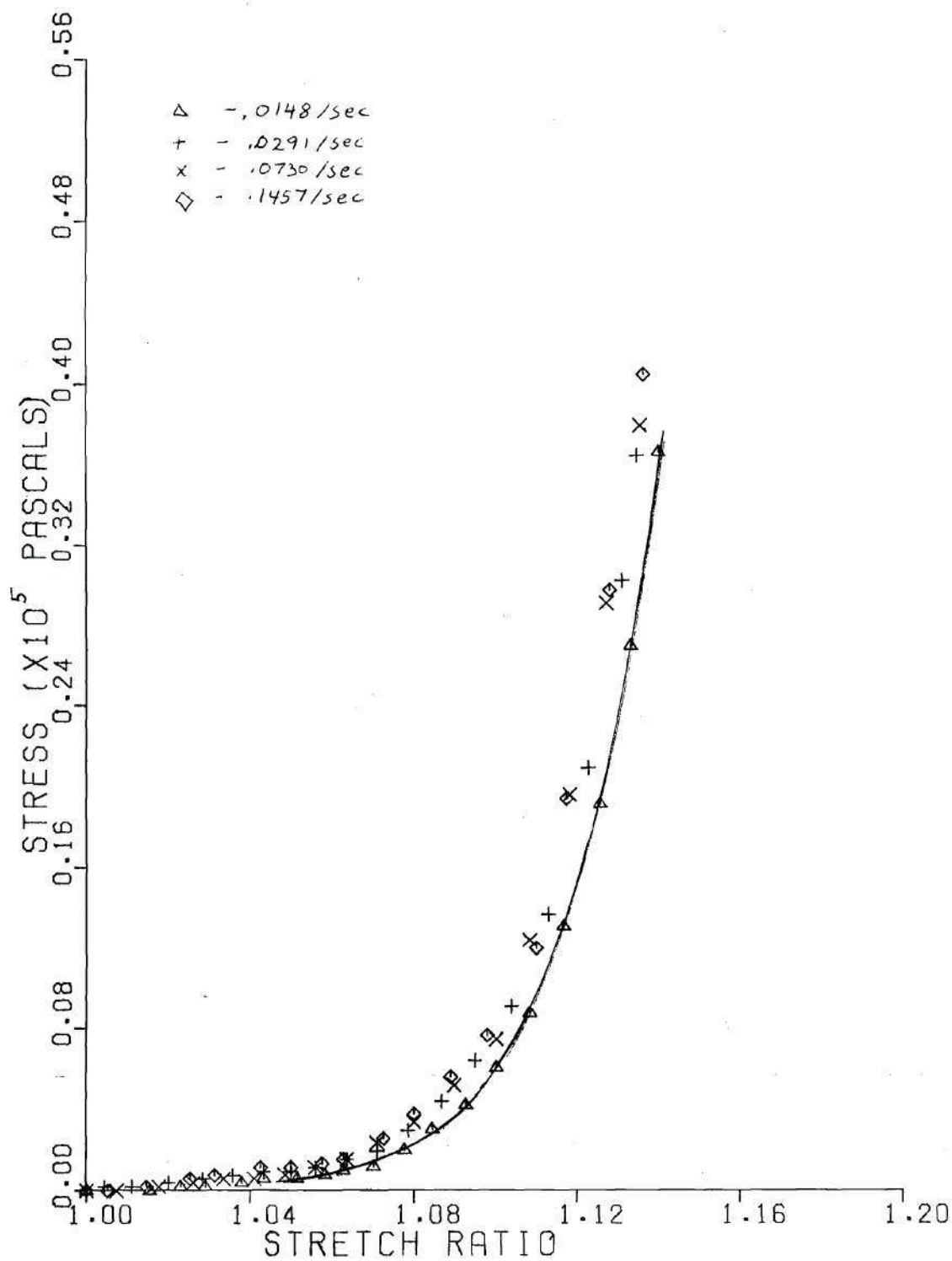


Figure A3. Effect of Strain Rate on Stress-Strain Curve - CF167

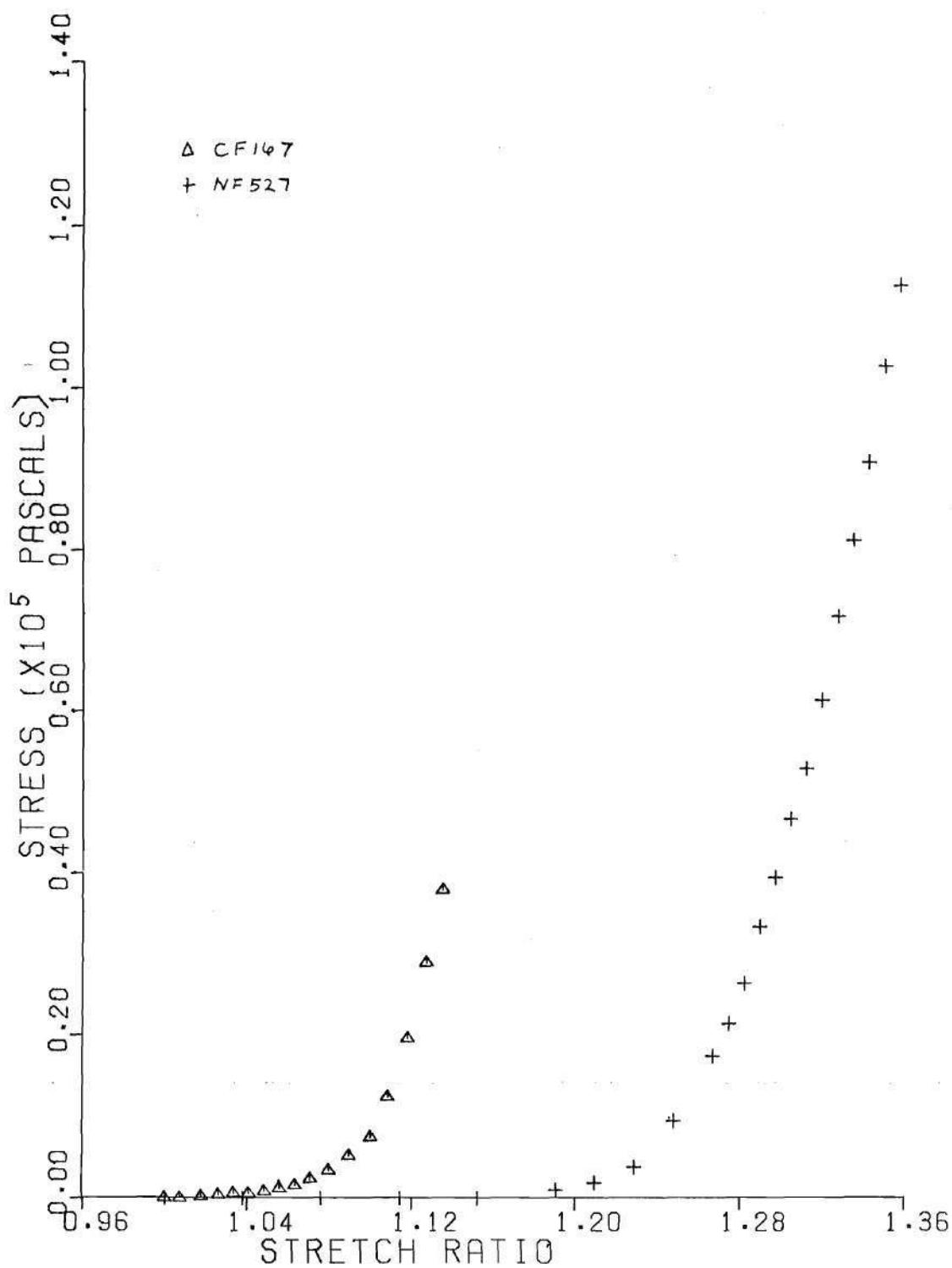


Figure A4. Stress versus Stretch Ratio - CF167 and NF527

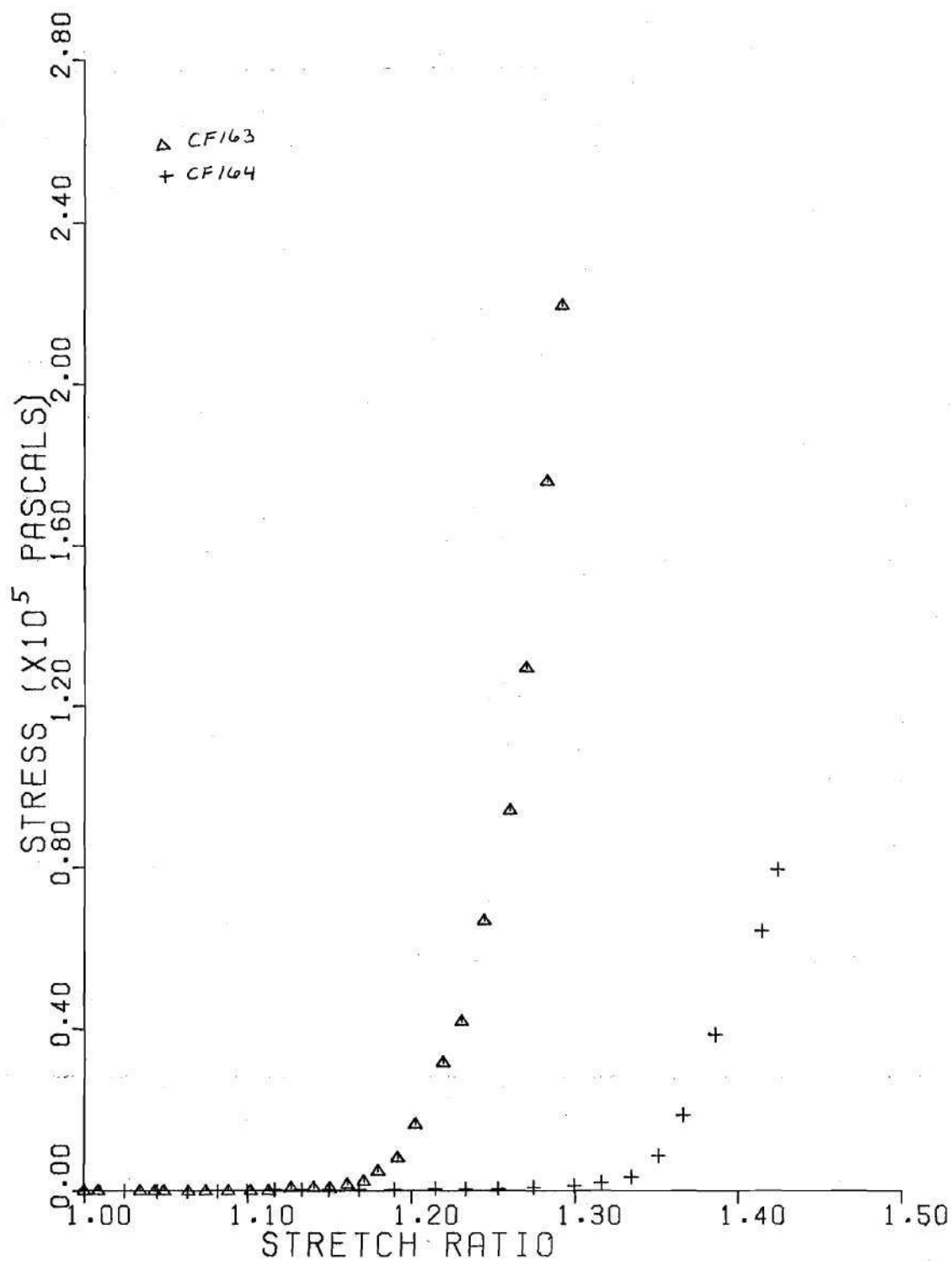


Figure A5. Stress versus Stretch Ratio - CF163 and CF164

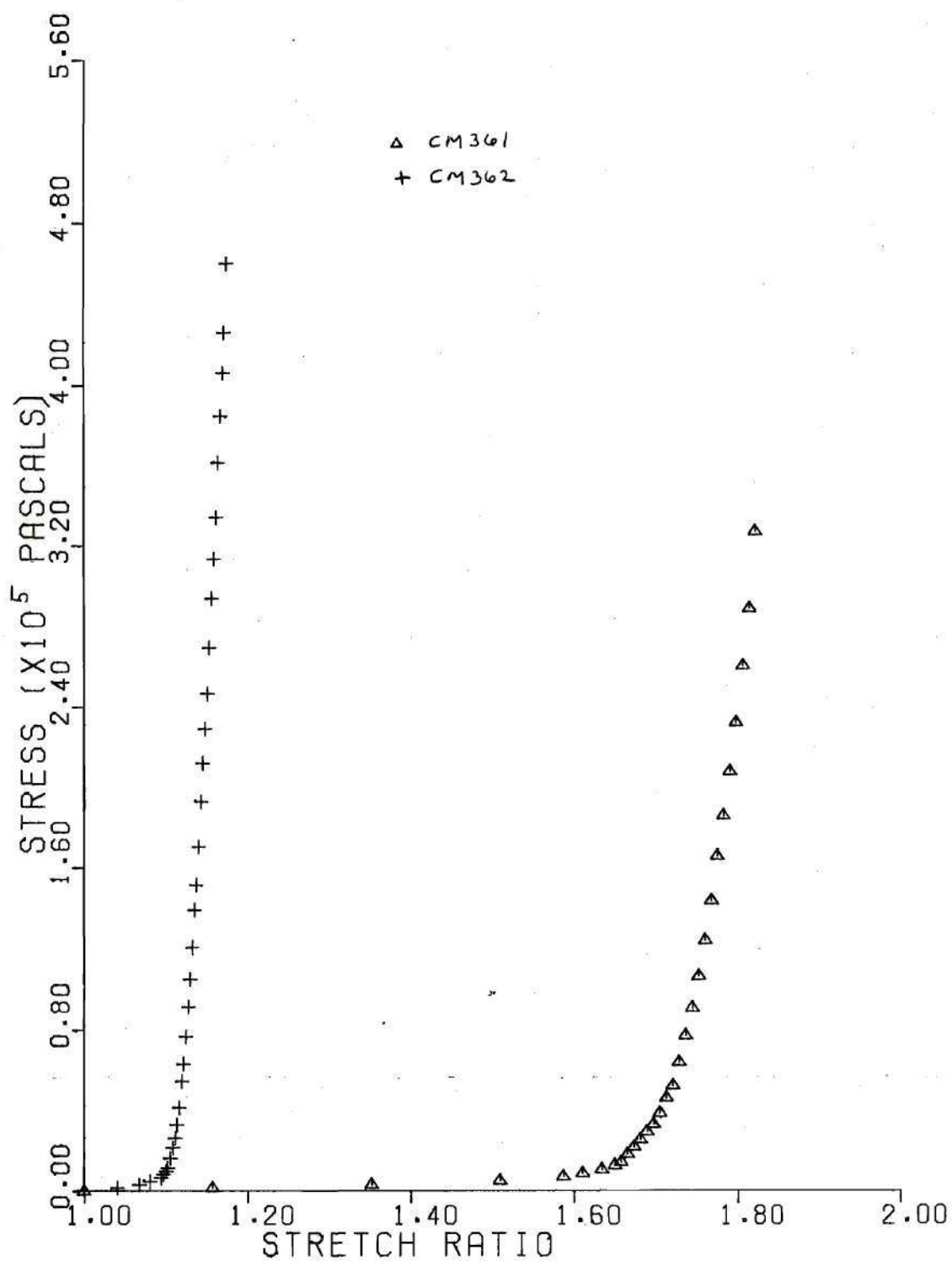


Figure A6. Stress versus Stretch Ratio - CM361 and CM362

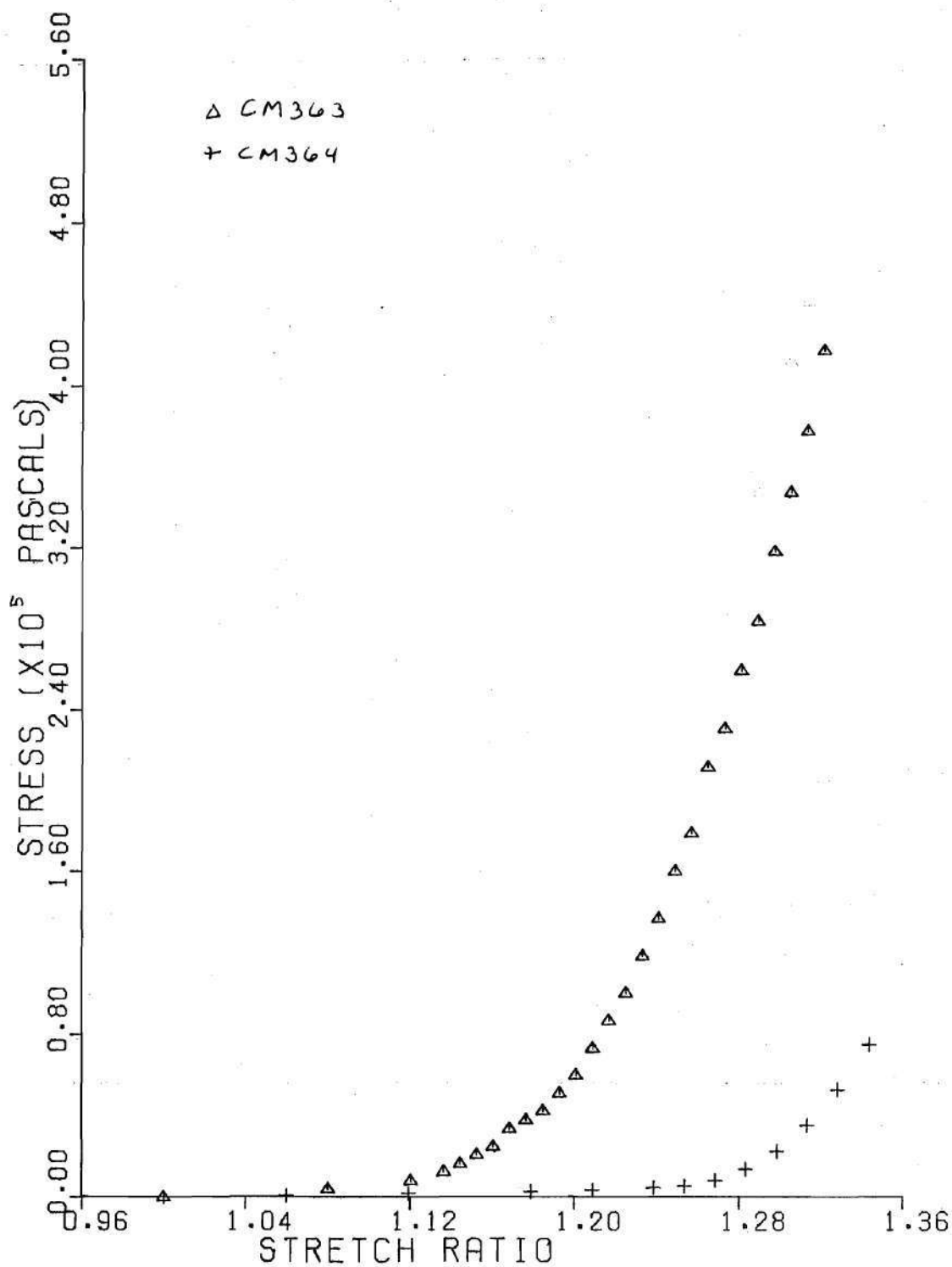


Figure A7. Stress versus Stretch Ratio - CM363 and CM364

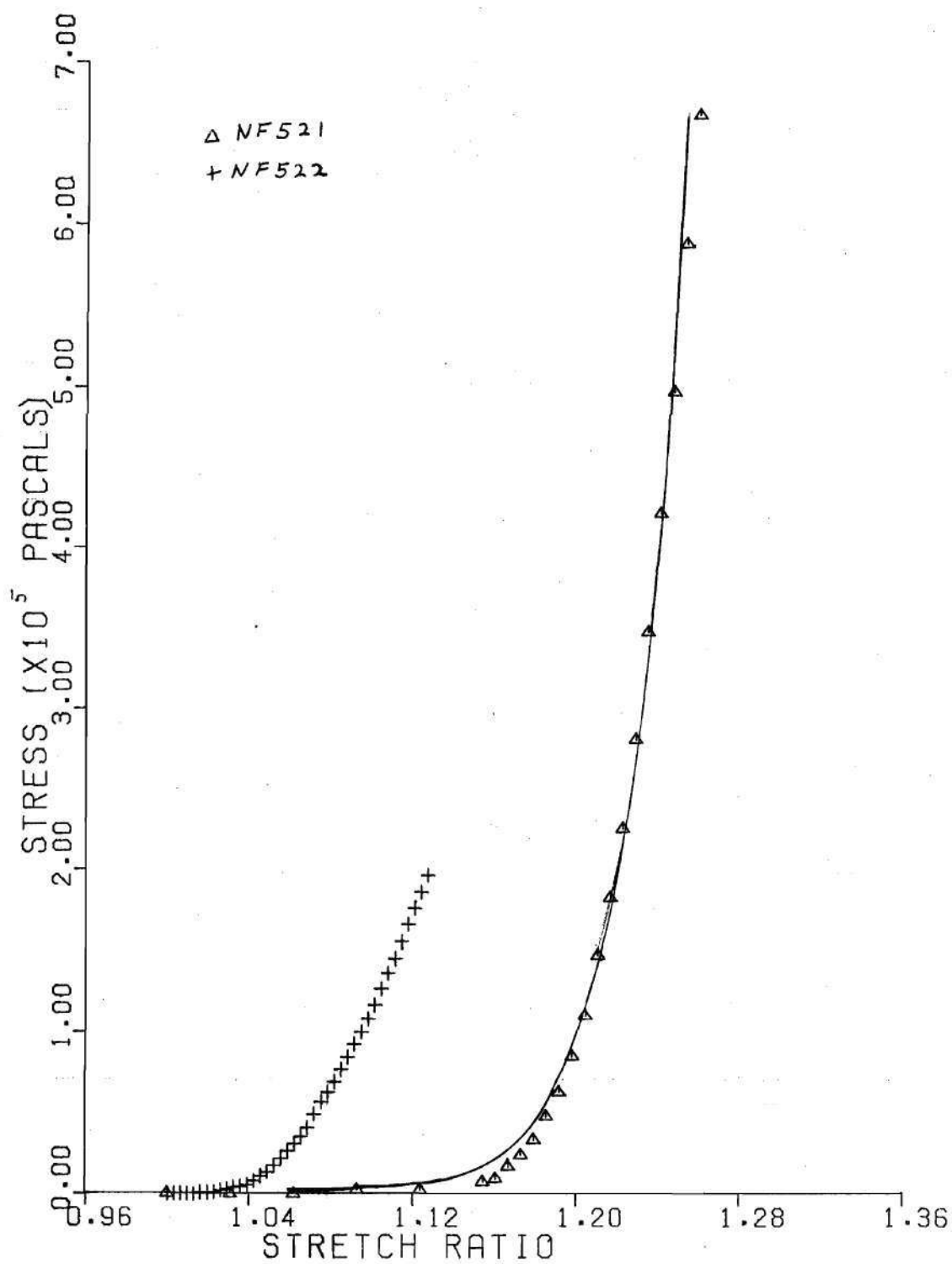


Figure A8. Stress versus Stretch Ratio - NF521 and NF522

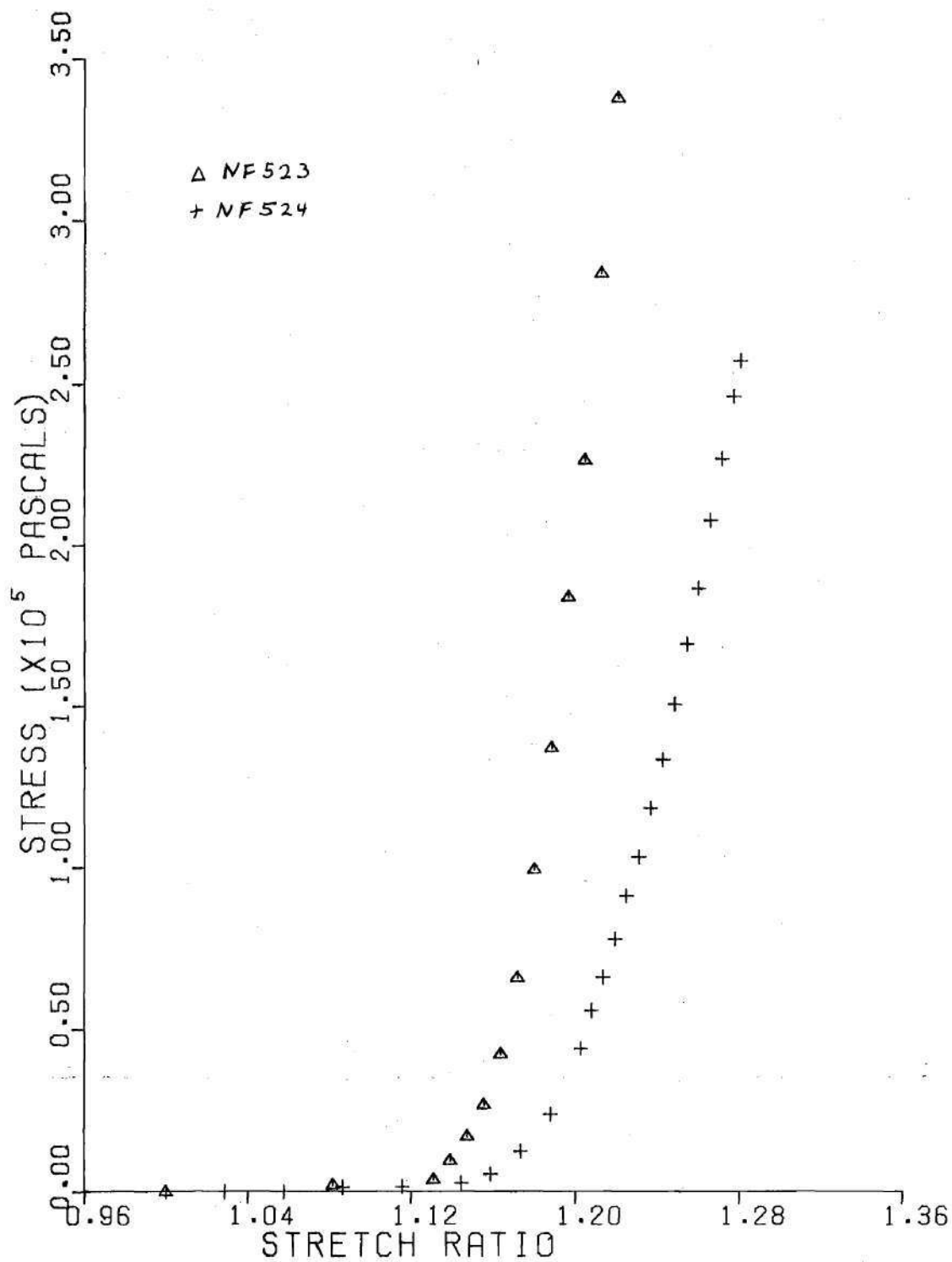


Figure A9. Stress versus Stretch Ratio - NF523 and NF524

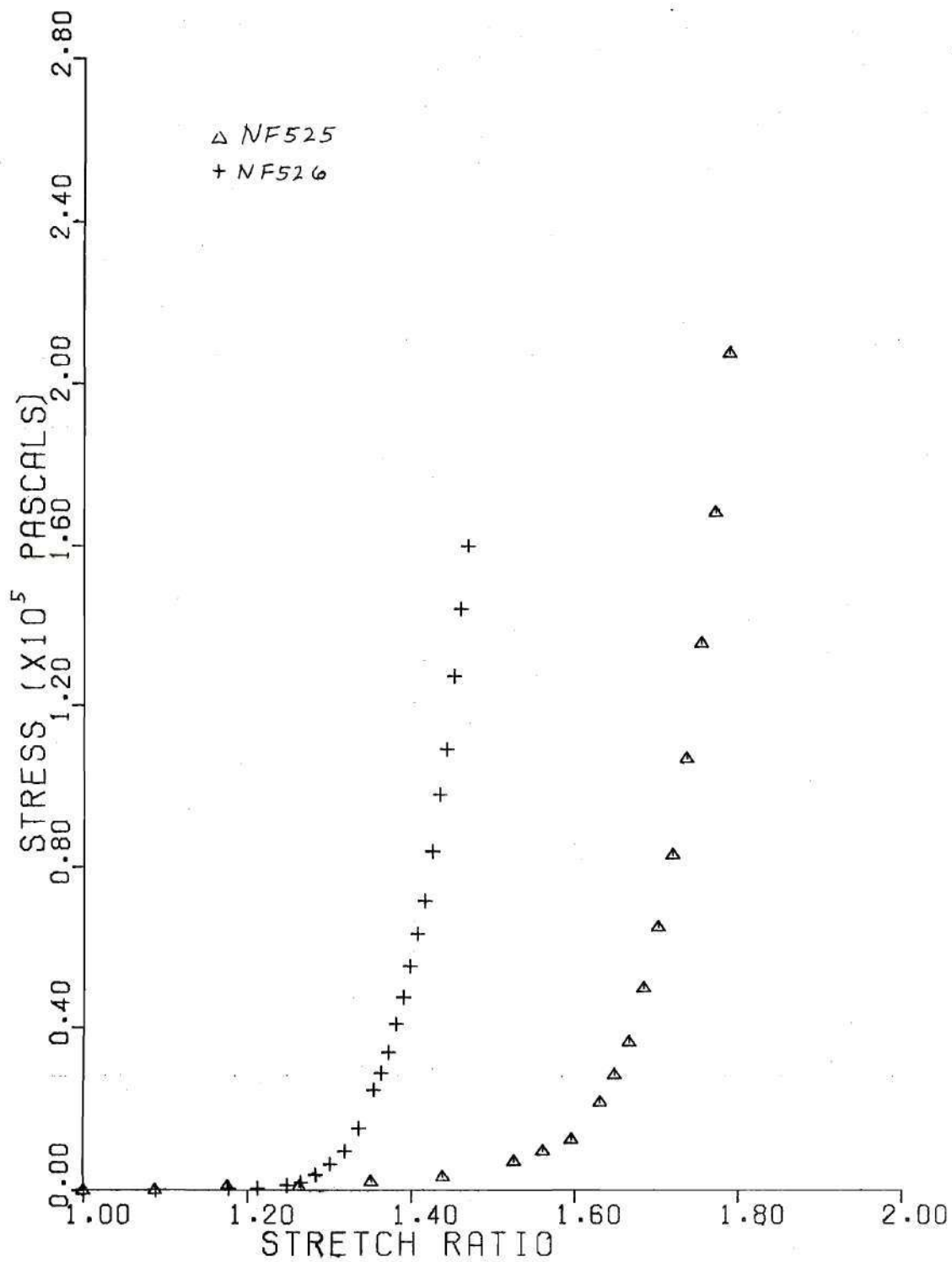


Figure A10. Stress versus Stretch Ratio - NF525 and NF526

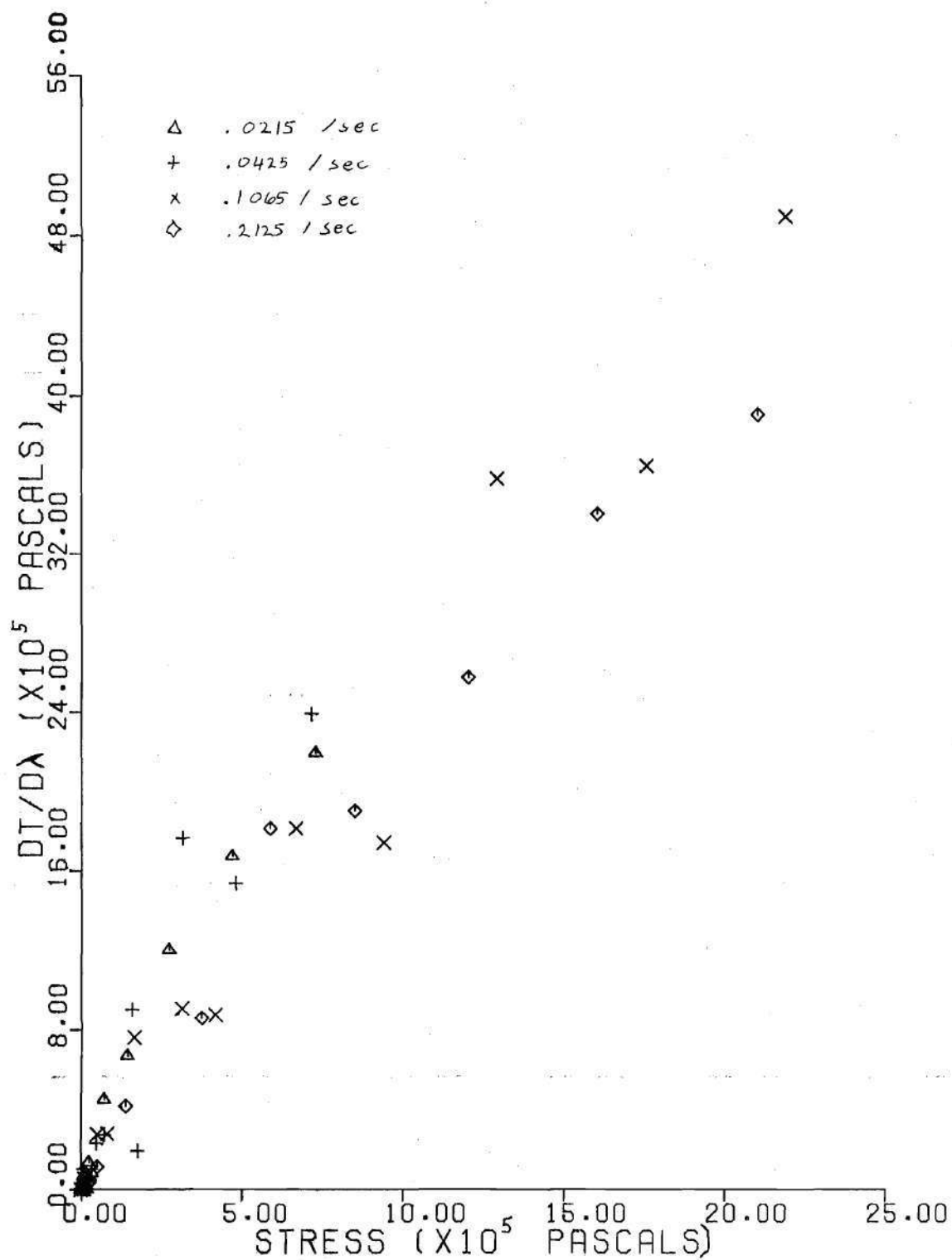


Figure A11. Secant Elastic Modulus versus Stress - CF163

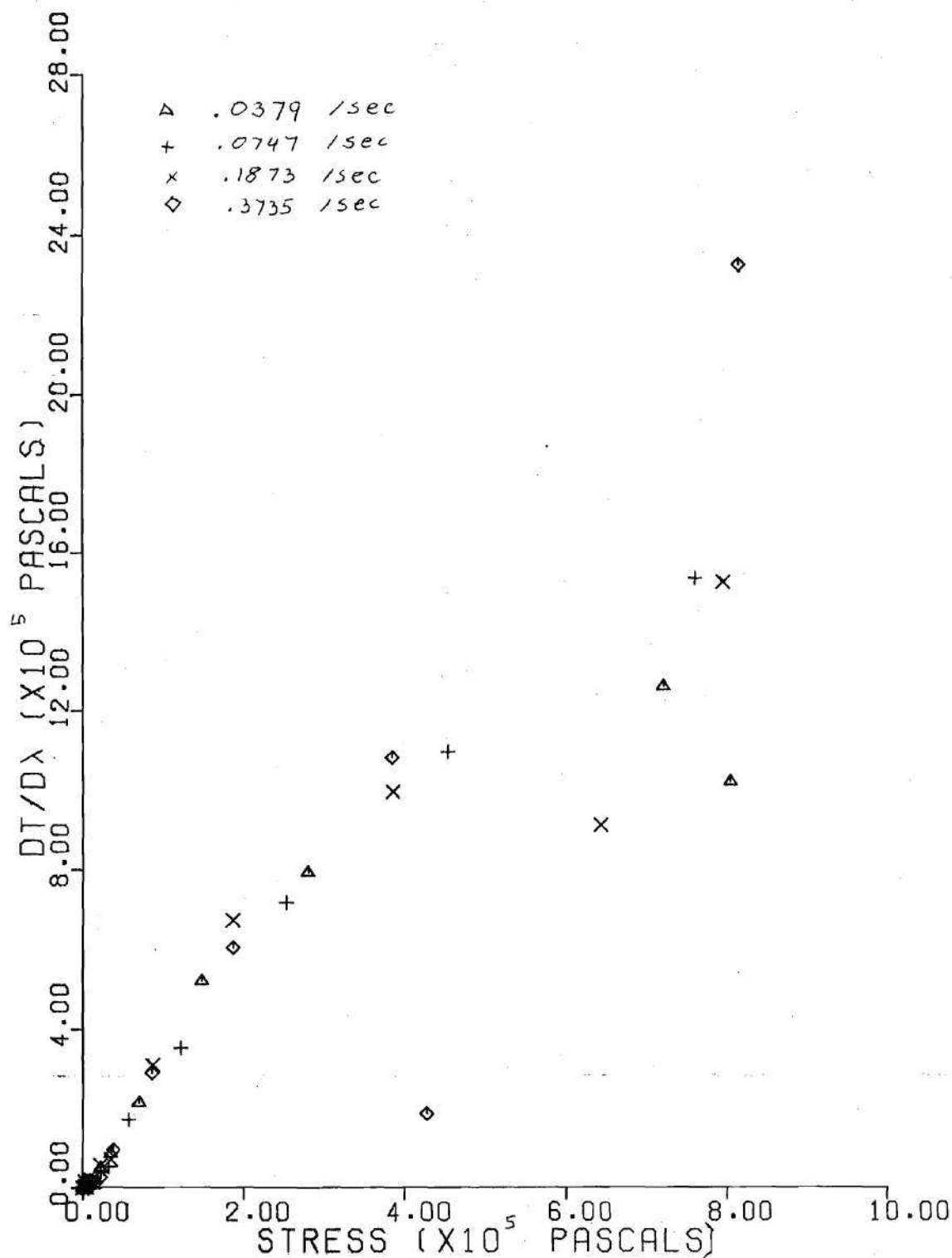


Figure A12. Secant Elastic Modulus versus Stress - CF164

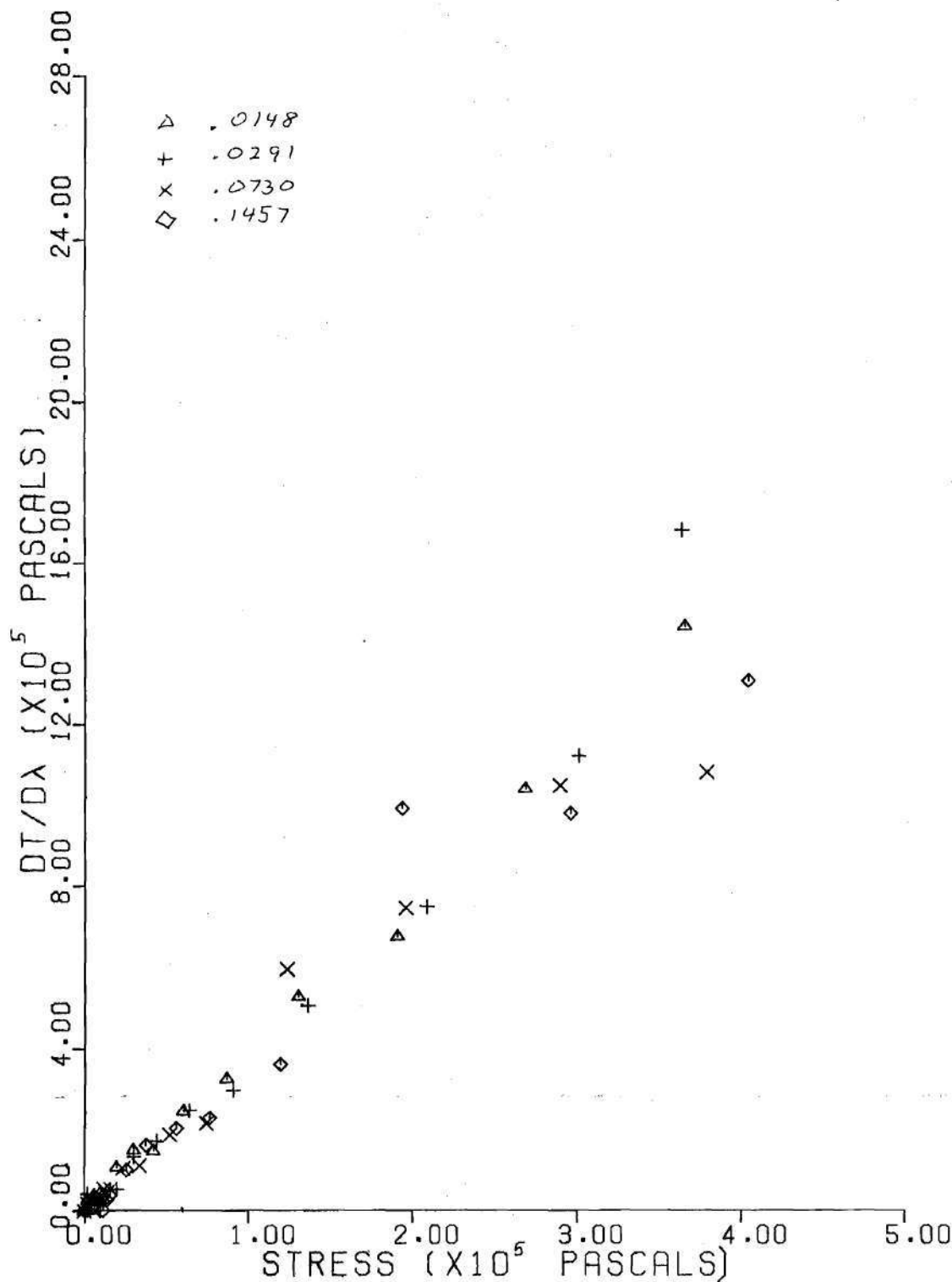


Figure A13. Secant Elastic Modulus versus Stress - CF167

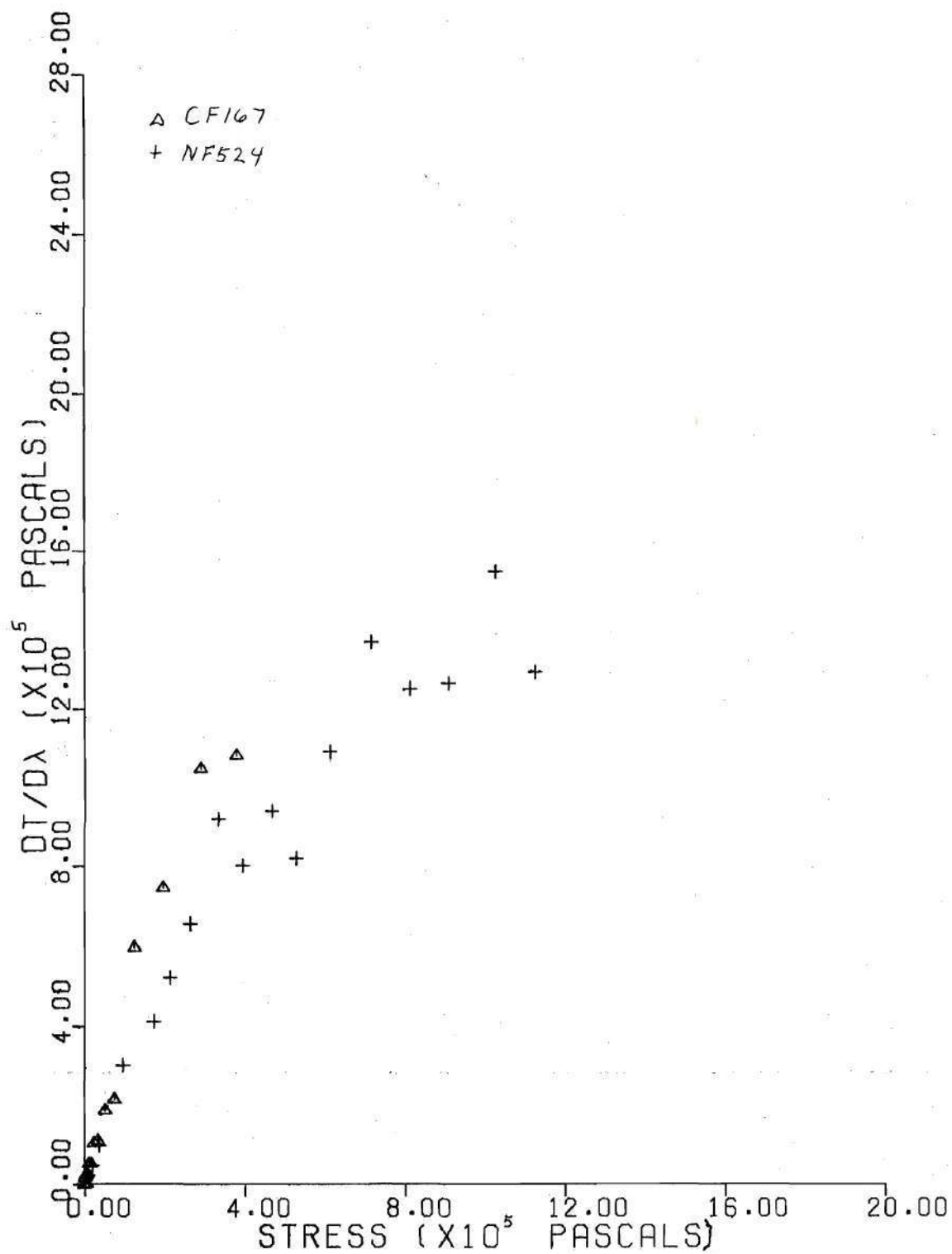


Figure A14. Secant Elastic Modulus versus Stress - CF167, NF527

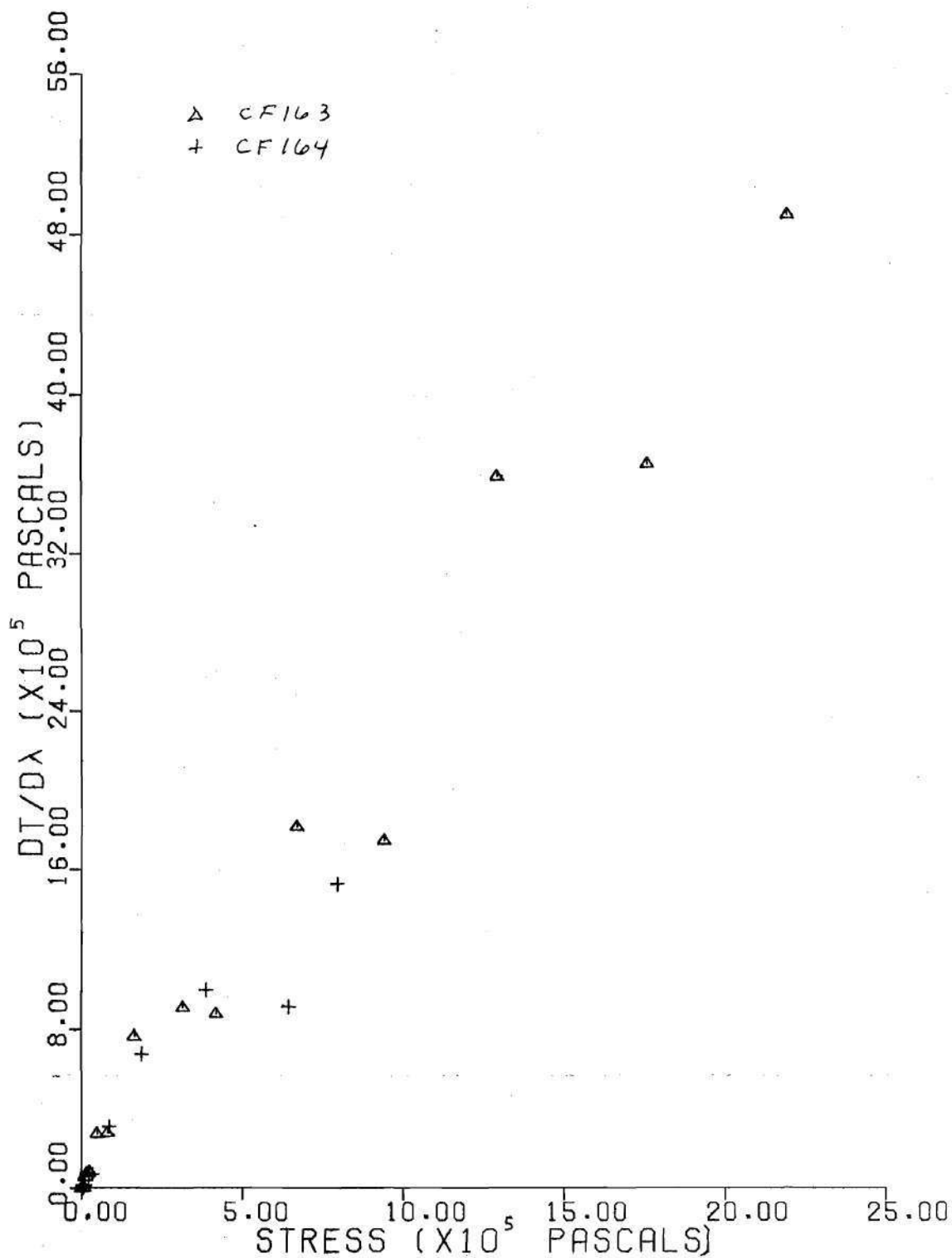


Figure A15. Secant Elastic Modulus versus Stress - CF163,CF164

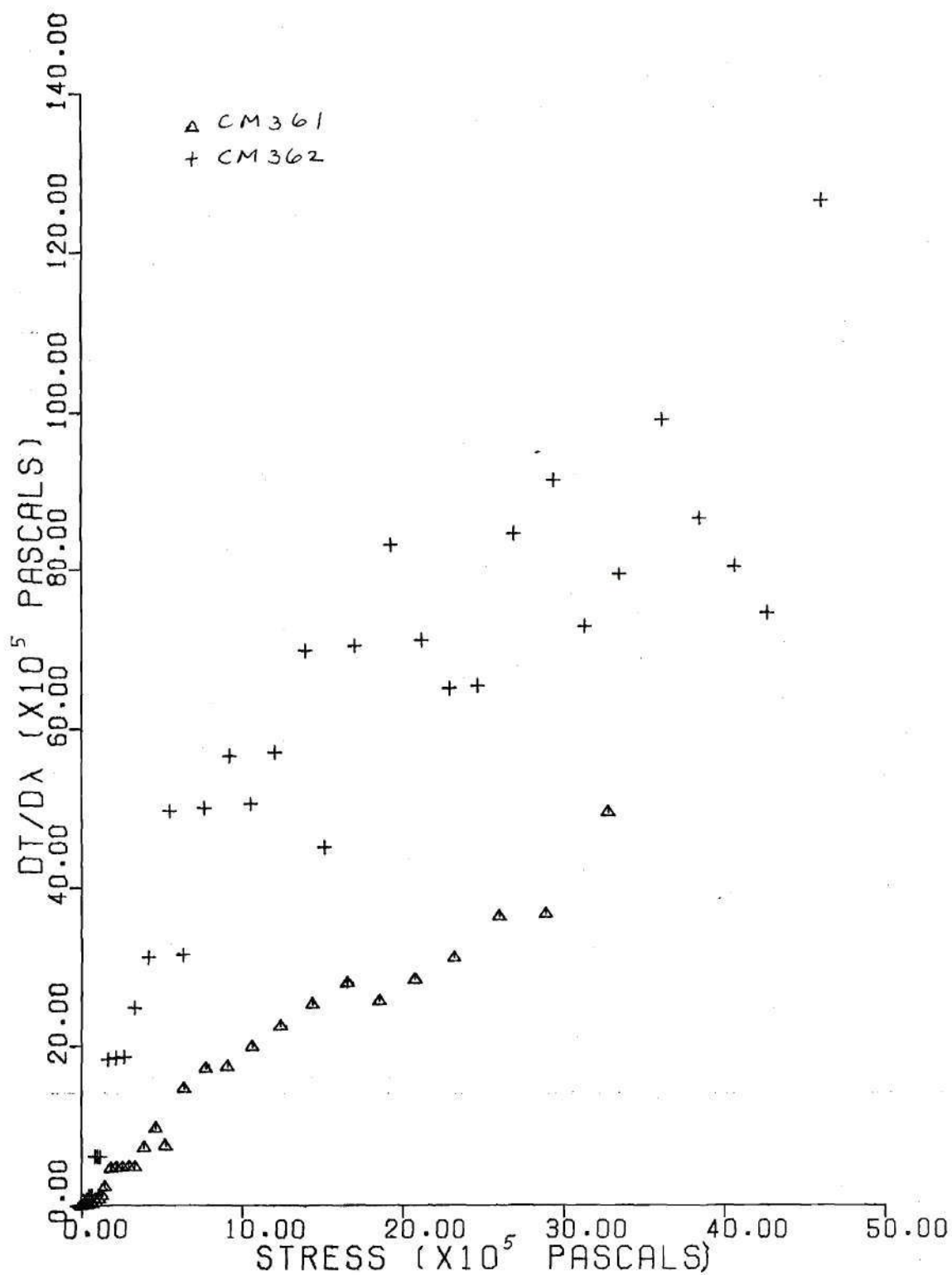


Figure A16. Secant Elastic Modulus versus Stress - CM361, CM362

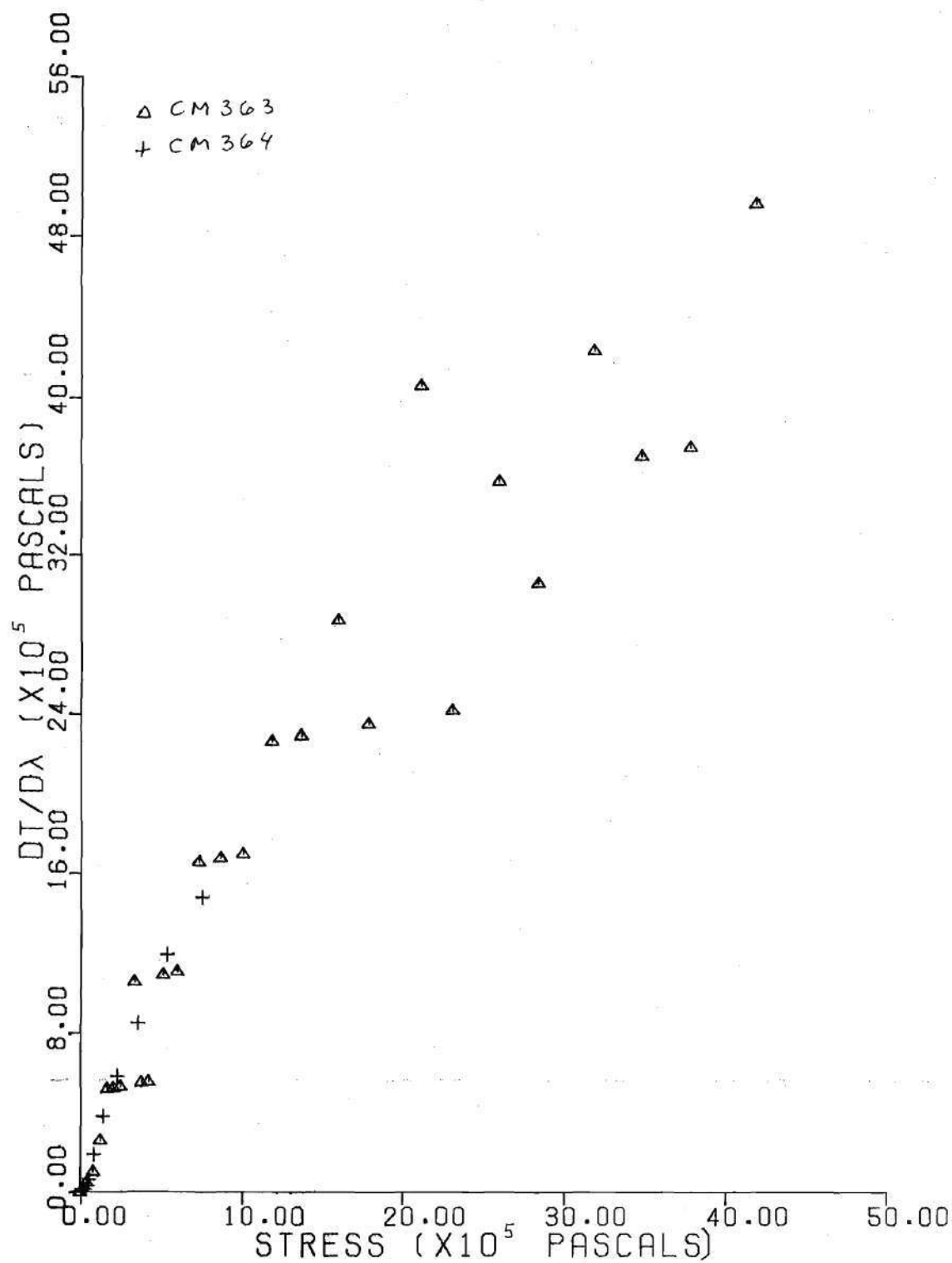


Figure A17. Secant Elastic Modulus versus Stress - CM363, CM364

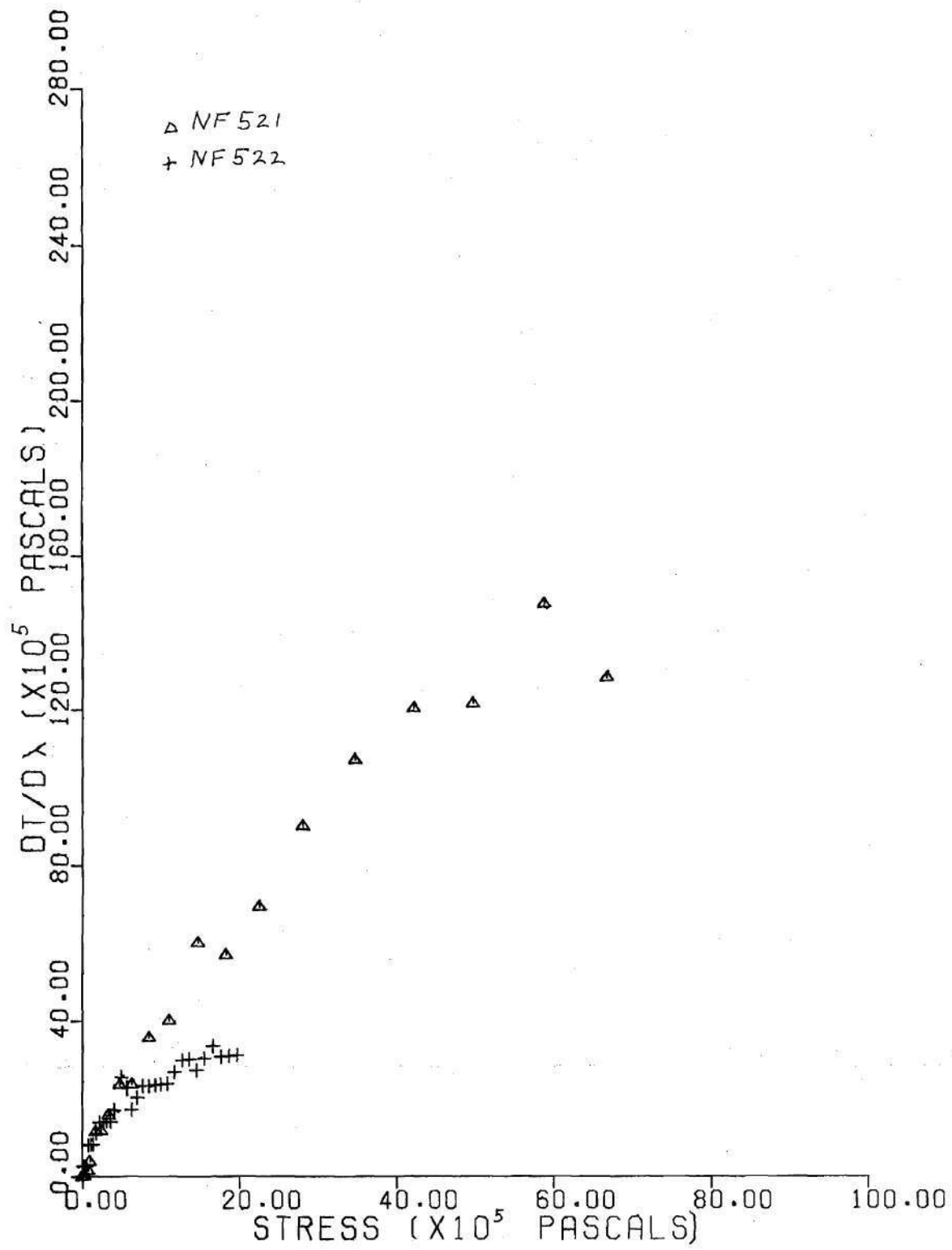


Figure A18. Secant Elastic Modulus versus Stress - NF521, NF522

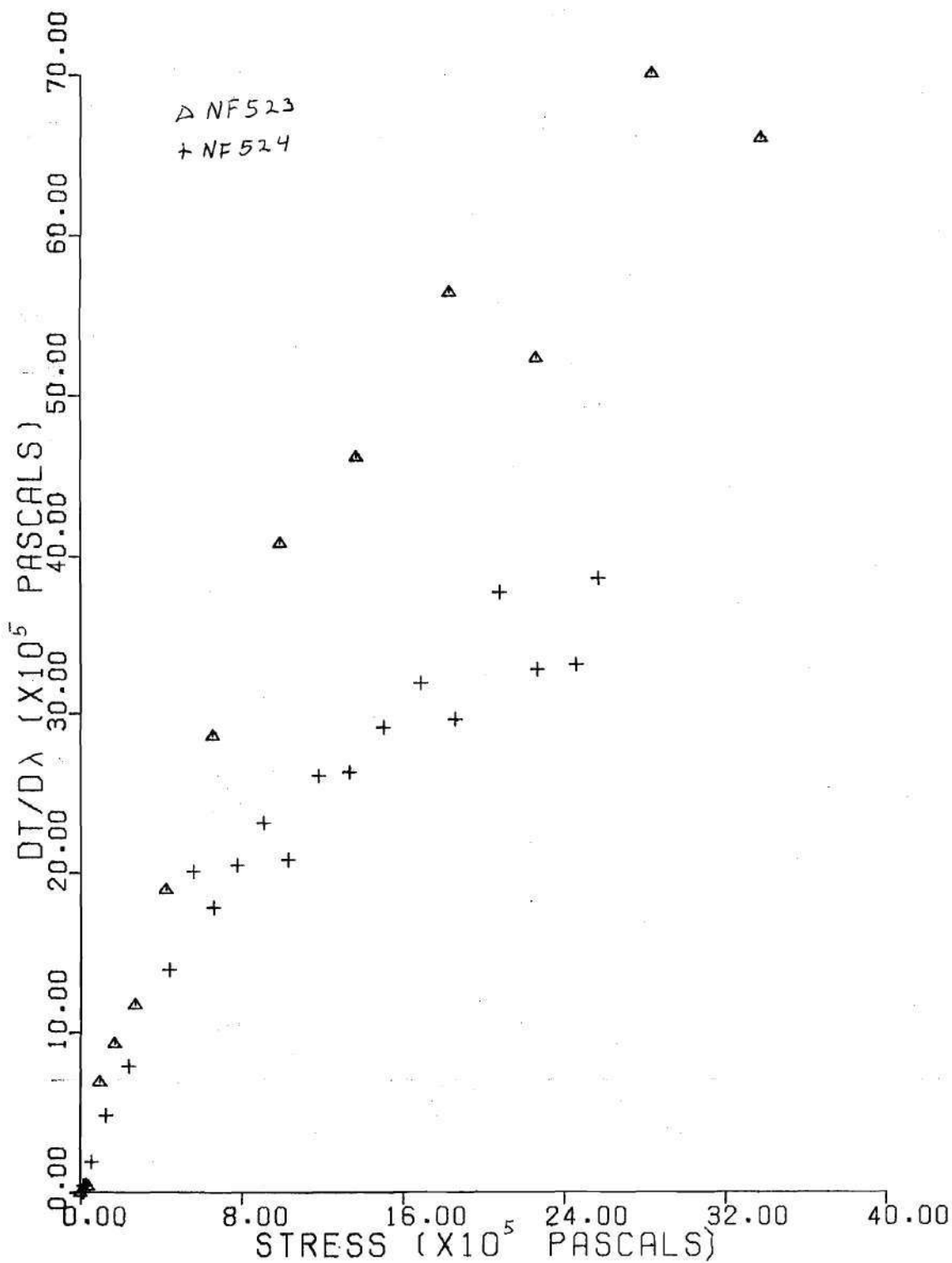


Figure A19. Secant Elastic Modulus versus Stress - NF523, NF524

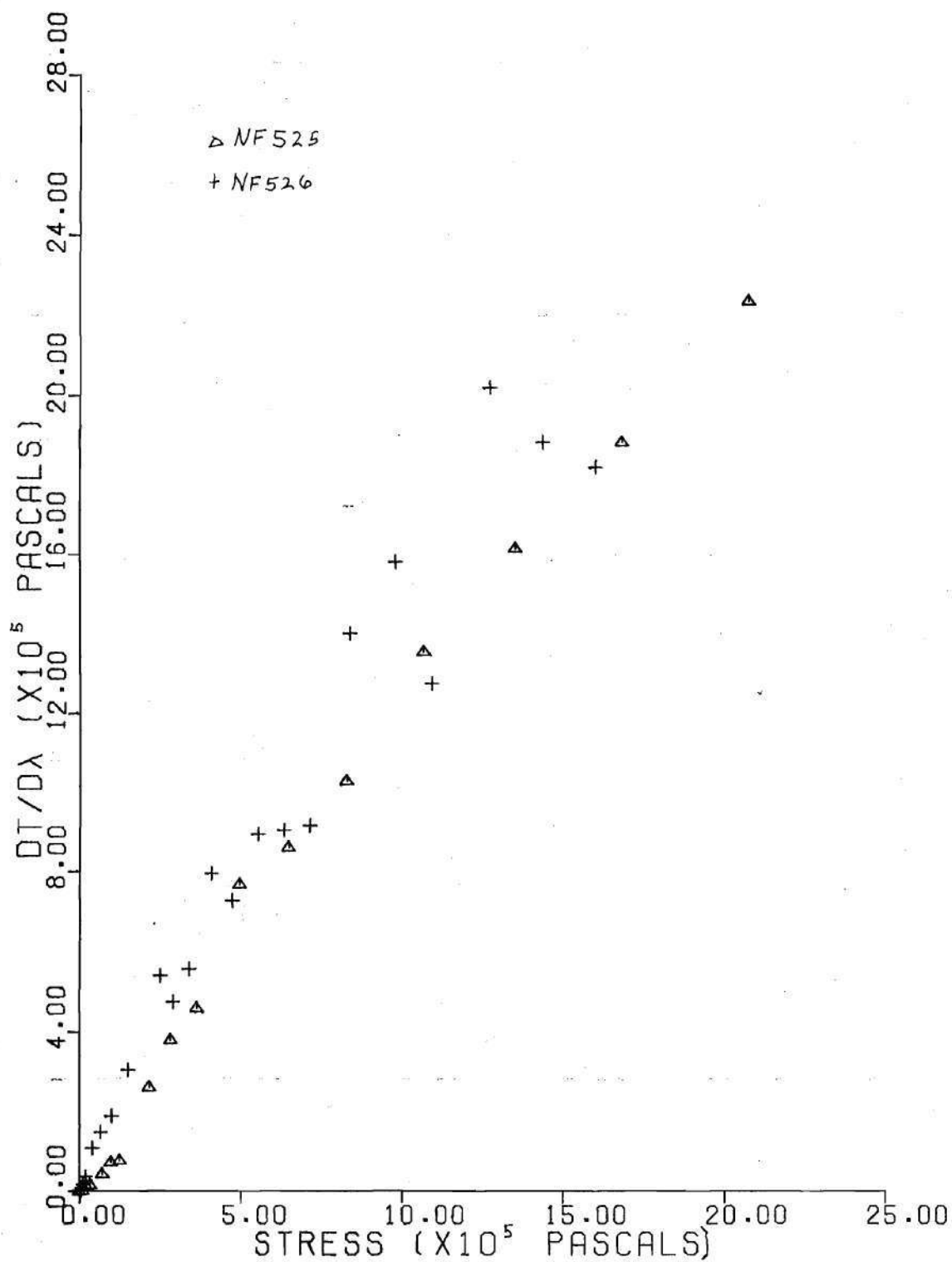


Figure A20. Secant Elastic Modulus versus Stress - NF525, NF526

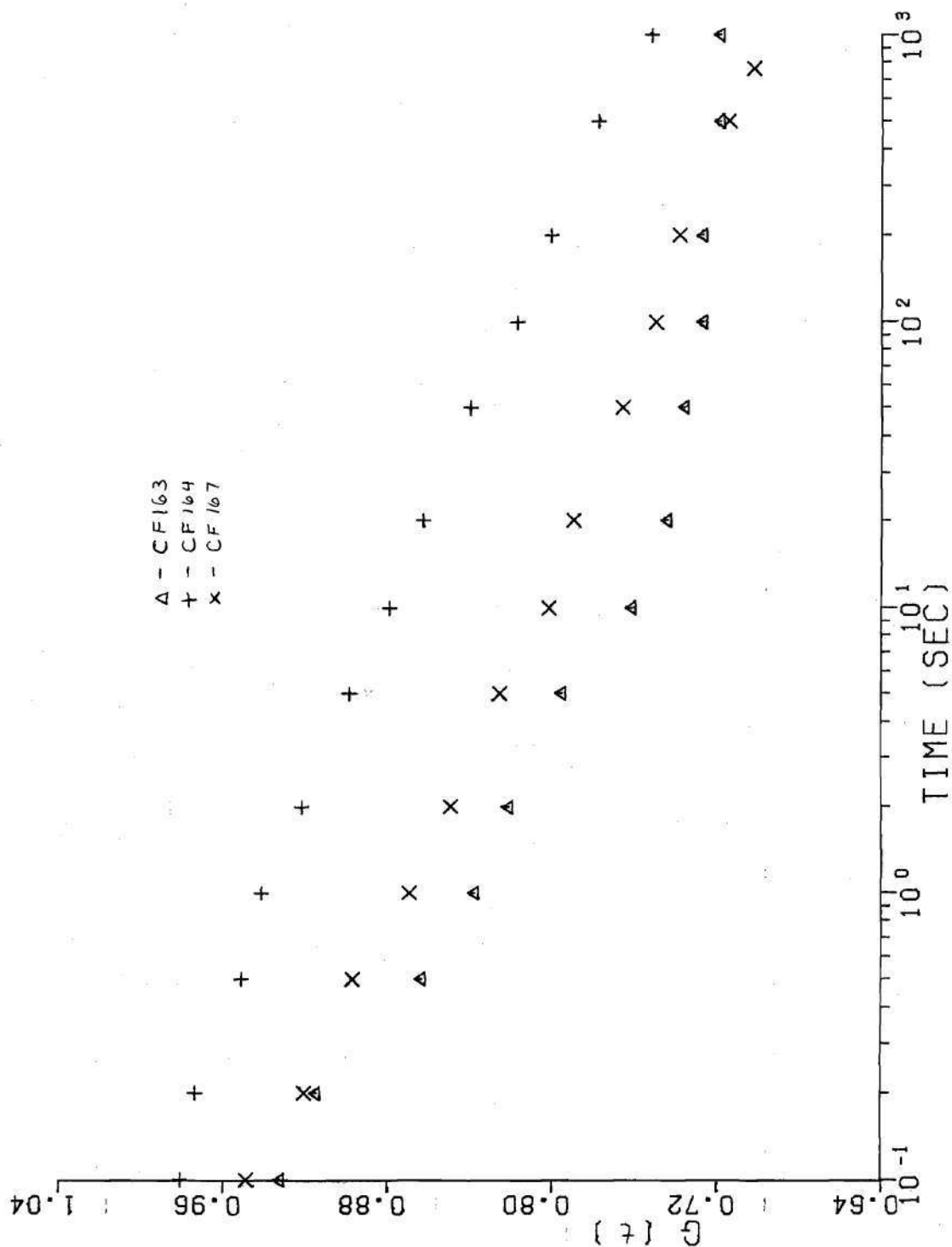


Figure A21. Reduced Relaxation Function - CF163, CF164, CF167

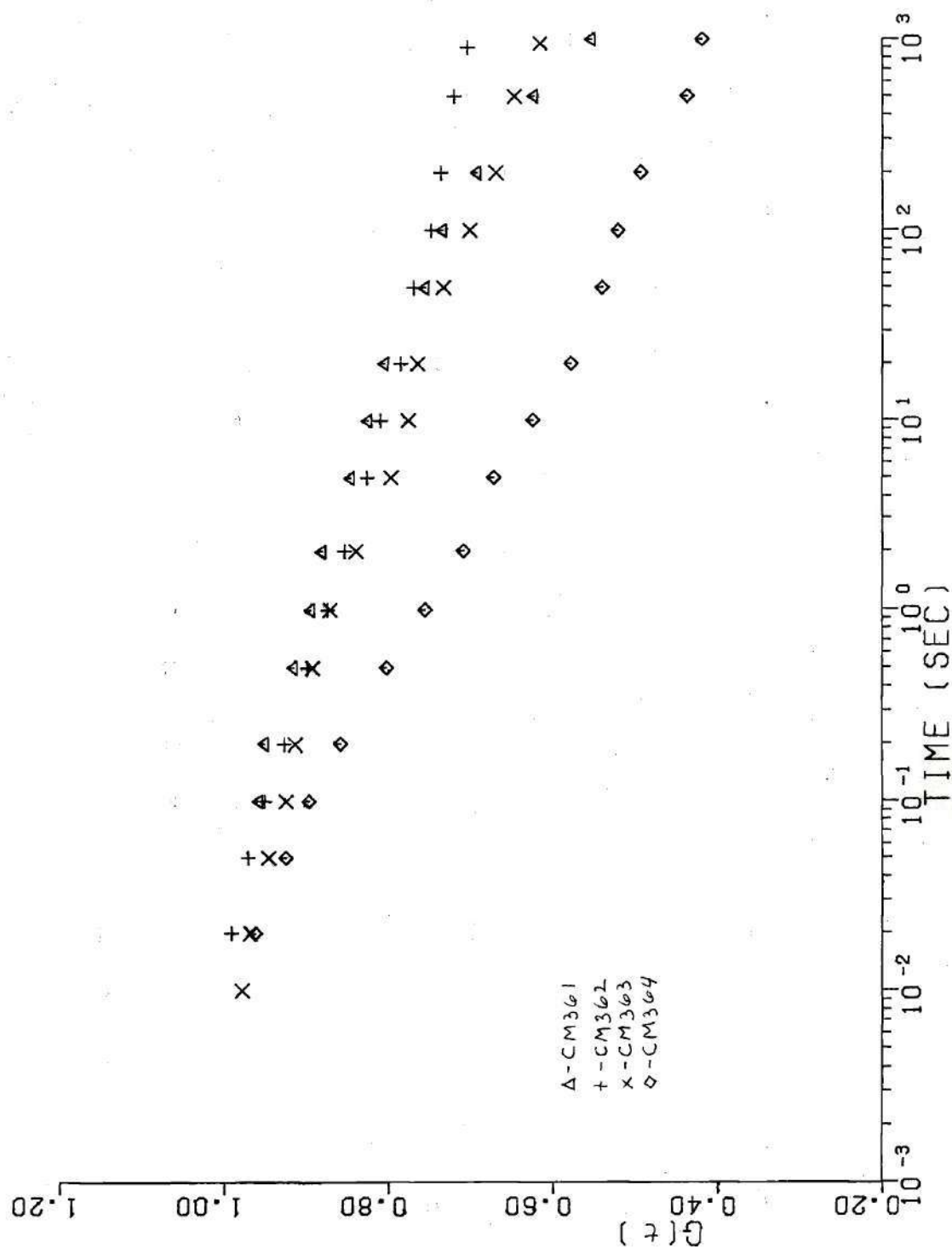


Figure A22. Reduced Relaxation Function -  
CM361, CM362, CM363, CM364

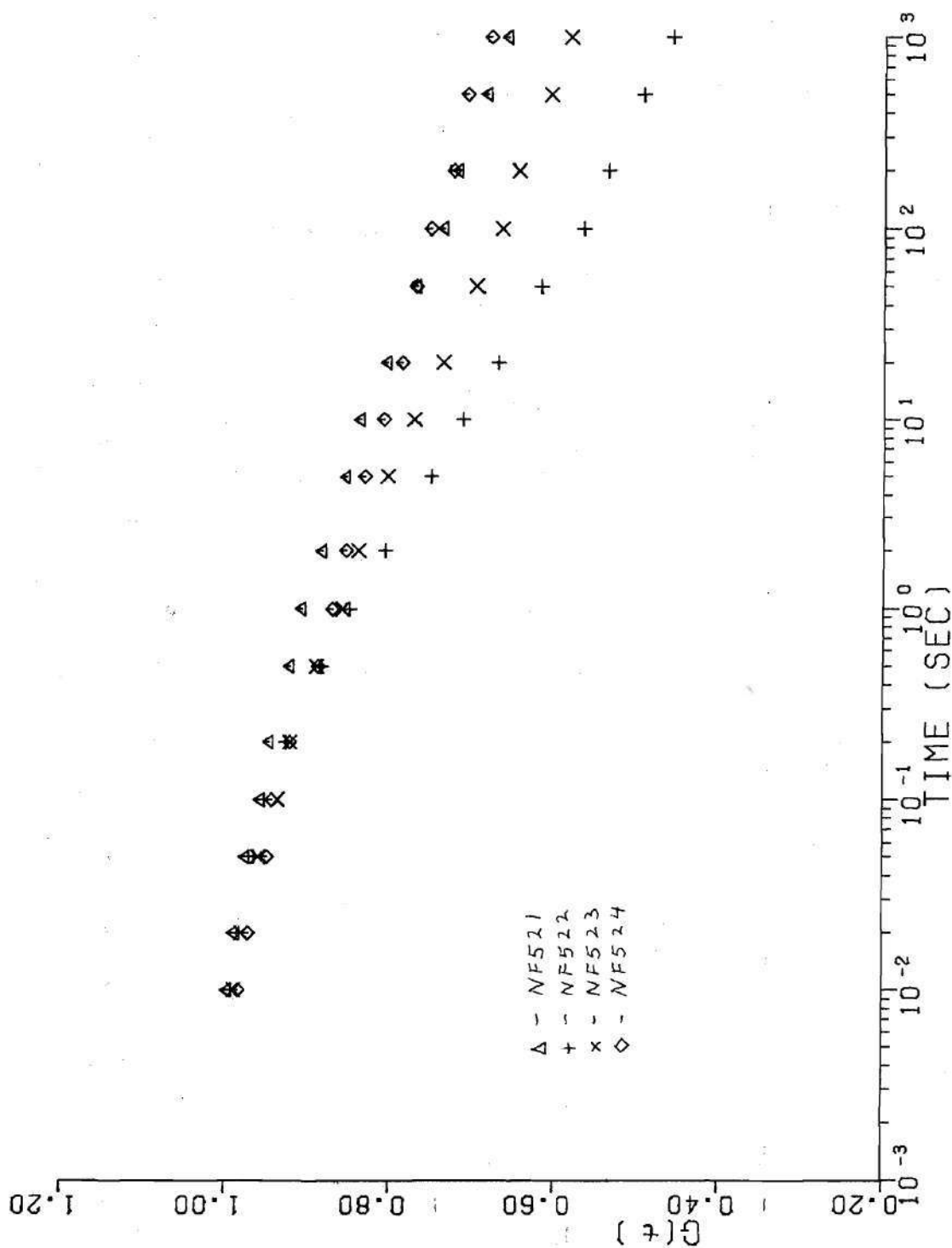


Figure A23. Reduced Relaxation Function -  
NF521, NF522, NF523, NF524

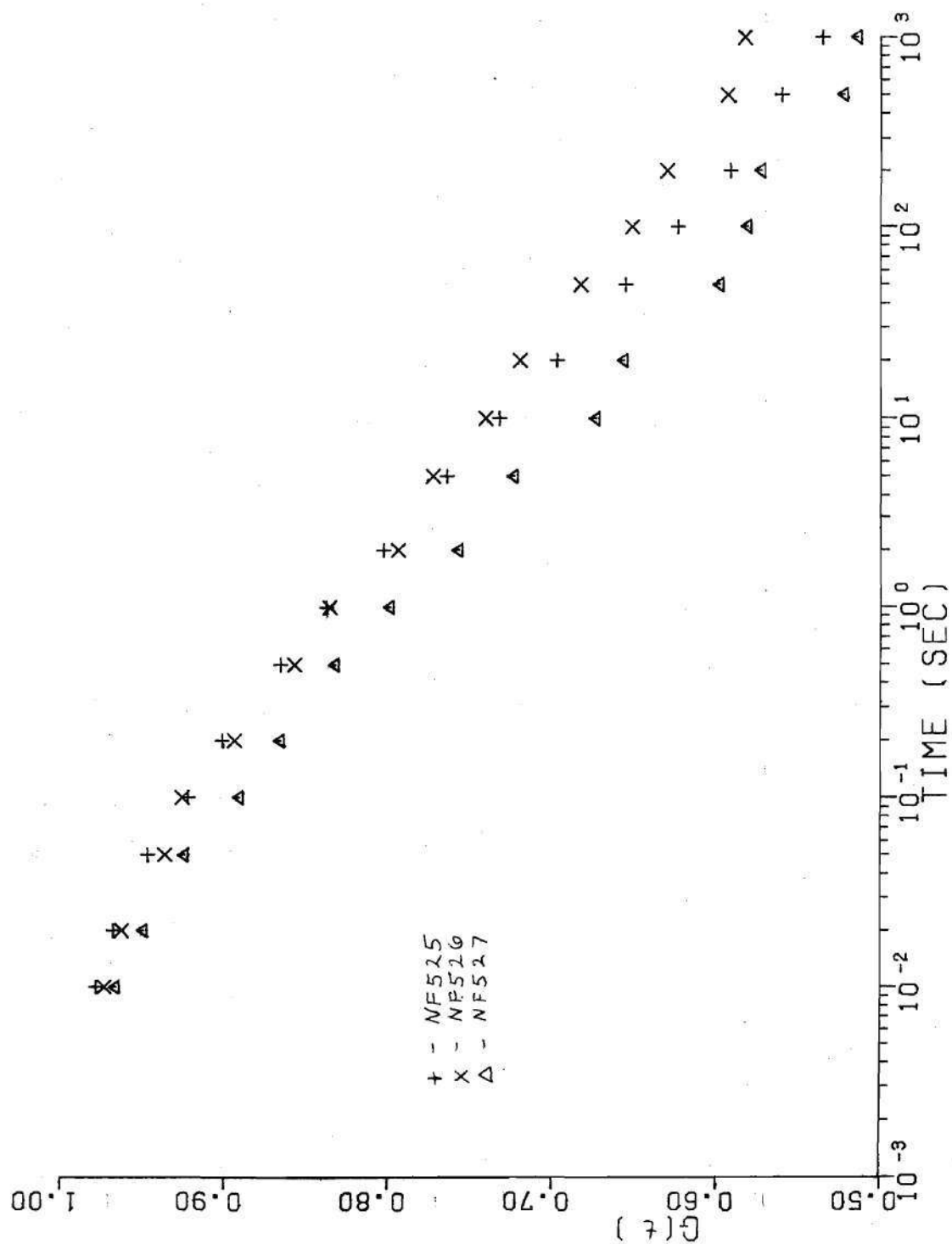


Figure A24. Reduced Relaxation Function - NF525,NF526,NF527

# BIBLIOGRAPHY

- [1] Baden, Wayne F., Ed., "Vaginal Relaxation", Clinical Obstetrics and Gynecology. 15, no. 4: 1033, 1972.
- [2] Berghaus, Donald G., "Fitting of Simple Approximation Functions Using Nonlinear Least-squares Methods", Experimental Mechanics. 17, no. 1: 14-20, 1977.
- [3] Black, Jonathan, "Dead or Alive: The Problem of In Vitro Tissue Mechanics", J. Biomed. Mater. Res. 10: 377-389, 1976.
- [4] Chen, H.Y.L., "Rabbit Mesentery as Viscoelastic Material --An Approach to the Mechanical Properties of Soft Tissues", Ph.D Thesis, University of California, San Diego, Ca., 1973.
- [5] Chen, H.Y.L. and Fung, Y.C., "Stress-Strain-History Relations of Rabbit Mesentery in Simple Elongation", Biomechanics Symposium, ASME, AMD-Vol.2: 9-10, 1973.
- [6] Fitzgerald, Edwin R., "Dynamic Mechanical Measurements During the Life to Death Transition in Animal Tissues", Biorheology. 12: 397-408, 1975.
- [7] Fung, Y.C.B., "Elasticity of Soft Tissues in Simple Elongation", Am.J of Physiology. 213: 1532, 1967.
- [8] Fung, Y.C.B., "Stress-strain-history Relations of Soft Tissues in Simple Elongation", Biomechanics : Its Foundations and Objectives, Ed. Fung, Y.C.B., Perrone, N. and Anliker, M., Prentice-Hall, Englewood Cliffs, N.J., 1972.
- [9] Fung, Y.C.B., "Biorheology of Soft Tissues", Biorheology. 10: 139-155, 1973.
- [10] Harkness, M.L.F., and Harkness, R.D., "The Use of Mechanical Tests in Determining the Structure of Connective Tissues", Biorheology. 10: 157-163, 1973.
- [11] Hart, R.T., "A Quantitative Study of the Mechanical Behavior of Endopelvic Fascia", M.S. Thesis, Georgia Institute of Technology, Atlanta, Ga., 1977.
- [12] Kenedi, R.M., Gibson, T., and Daly, C.H., "Bioengineering Studies of the Human Skin, the Effect of

Unidirectional Tension", Structure And Function of Connective and Skeletal Tissue. Ed. Jackson, S.M., Tristram, G.R., St. Andrews, Scotland: Scientific Committee, 388-395, 1964.

[13] Ko, F.K.F., "Nonlinear Viscoelasticity of Polyamide Fibers", Georgia Institute of Technology, Atlanta, Ga., 1976.

[14] Marangoni, R.D., Glaser, A.A., Must, J.S., Brody, G.S., Beckwith, T.G., Walker, G.R., and White, W.L., "Effect of Storage and Handling Techniques on Skin Tissue Properties", Annals New York Academy of Sciences. pp. 441-453, 1966.

[15] Mathews, Larry S., and Ellis, Donald, "Viscoelastic Properties of Cat Tendon: Effects of Time After Death and Preservation By Freezing", J. Biomechanics. 1:65-71, 1968.

[16] Rabkin, Simon W. and Hsu, Ping Hwa, "Mathematical and Mechanical Modeling of Stress-Strain Relationship of Pericardium", Am. J. of Physiology. 229, no. 4: 896-900, 1975.

[17] Richardson, A.C., Lyon, J.B. and Williams, N.L., "A New Look at Pelvic Relaxation", Am. J. of Obstet. and Gynec. 126: 568, 1976.

[18] Richardson, A.C., Shemlock, B. and Williams, N.L., "Pelvic Supports, Dynamic Structures?", in press.

[19] Smith, J.W., "The Elastic Properties of the Anterior Cruciate Ligament of the Rabbit", J. of Anatomy. 88, no. 3: 369-380, 1954.

[20] Sonnenblick, E.H., "Series Elastic and Contractile Elements in Heart Muscle; Change in Muscle Length", Amer. J. Physiol. 297: 1330, 1964.

[21] Van Brocklin, J.D., and Ellis, D.G., "A Study of the Mechanical Behavior of Toe Extensor Tendons Under Applied Stress", Archives of Physical Medicine and Rehabilitation. 46: 369-373, 1965.

[22] Viidik, A., Sandqvist, L., and Magi, M., "Influence of Postmortal Storage on Tensile Strength Characteristics and Histology of Rabbit Ligaments", Acta Orthopaedica Scandinavica, Supplementum 79. pp. 7-38, 1965.

[23] Viidik, A., and Lewin, T., "Changes in Tensile Strength Characteristics and Histology of Rabbit Ligaments Induced by

Different Modes of Postmortal Storage", Acta Orthopaedica Scandinavica. 37: 141-155, 1966.

[24] Viidik, A., "Functional Properties of Collagenous Tissues", Int. Rev. Connective Tissue Res. 6: 127, 1973.